eISSN 2005-5447
International Journal of Stem Cells Vol. 10, No. 2, 2017 https://doi.org/10.15283/ijsc17036

ORIGINAL ARTICLE

Proteomic Analysis of Human Adipose Derived Stem Cells during Small Molecule Chemical Stimulated Pre-neuronal Differentiation

Jerran Santos[1,2], Bruce K Milthorpe[1], Benjamin R Herbert[3], Matthew P Padula[2]

[1]*Advanced Tissue Regeneration & Drug Delivery Group, School of Life Sciences, University of Technology Sydney, NSW, Australia*
[2]*Proteomics Core Facility, School of Life Sciences, University of Technology Sydney, NSW, Australia*
[3]*Northern Clinical School, Sydney Medical School, University of Sydney, NSW, Australia*

Background: Adipose derived stem cells (ADSCs) are acquired from abdominal liposuction yielding a thousand fold more stem cells per millilitre than those from bone marrow. A large research void exists as to whether ADSCs are capable of transdermal differentiation toward neuronal phenotypes. Previous studies have investigated the use of chemical cocktails with varying inconclusive results.
Methods: Human ADSCs were treated with a chemical stimulant, beta-mercaptoethanol, to direct them toward a neuronal-like lineage within 24 hours. Quantitative proteomics using iTRAQ was then performed to ascertain protein abundance differences between ADSCs, beta-mercaptoethanol treated ADSCs and a glioblastoma cell line.
Results: The soluble proteome of ADSCs differentiated for 12 hours and 24 hours was significantly different from basal ADSCs and control cells, expressing a number of remodeling, neuroprotective and neuroproliferative proteins. However toward the later time point presented stress and shock related proteins were observed to be up regulated with a large down regulation of structural proteins. Cytokine profiles support a large cellular remodeling shift as well indicating cellular distress.
Conclusion: The earlier time point indicates an initiation of differentiation. At the latter time point there is a vast loss of cell population during treatment. At 24 hours drastically decreased cytokine profiles and overexpression of stress proteins reveal that exposure to beta-mercaptoethanol beyond 24 hours may not be suitable for clinical application as our results indicate that the cells are in trauma whilst producing neuronal-like morphologies. The shorter treatment time is promising, indicating a reducing agent has fast acting potential to initiate neuronal differentiation of ADSCs.

Keywords: Adult Stem Cells, Adipose, Neuronal, Proteomics, Cytokines

Introduction

Regenerative and translational medicine is a rapidly expanding area made possible by the availability of an abundant source of adipose derived stem cells (ADSCs) from lipoaspirates, less abundant bone marrow derived stem cells (BMSCs) and induced pluripotent stem cells (iPSCs). The need for regenerative therapies in osteogenesis and chondrogenesis has increased interest in transdifferentiation of these cells for autologous transplants and therapy development (1). Not surprisingly, neuronal regeneration and repair therapies are of great interest because of its potential to reverse injuries that have severe effects on quality

Accepted for publication July 4, 2017, Published online November 30, 2017
Correspondence to **Jerran Santos**
Faculty of Science, University of Technology Sydney, Office 04.07.430, Building 4 Cnr Thomas and Harris Streets, Ultimo 2007, NSW, Australia
Tel: +61-2-9514-8374, Fax: +61-2-9514-8206
E-mail: Jerran.Santos@uts.edu.au

of life (2, 3).

The generation of differentiated neuronal cells from progenitor stem cells has been attempted by a number of researchers over the last decade (4-6). Several have reported the successful passage of ADSCs and BMSCs, *in vitro* and *in vivo*, in the presence of simple chemicals and/or growth factors, such as beta-mercaptoethanol (BME) (7, 8), retinoic acid (RA) (9), dimethylsulfoxide (DMSO) and Butylated hydroxianisole (BHA), to rapidly differentiate morphologically toward a neuronal linage. The resultant cell populations have been shown to express morphological and protein surface marker identities consistent with that seen in primary derived neuronal tissue and cultured neuronal cell lines.

BME is a reducing agent and has been shown to be toxic to certain cell types when presented in concentrations higher than the micromolar range (10). The potential for BME to be used as an inducing agent for neuronal differentiation has been studied in a limited capacity (4, 5) and shown to rapidly cause differentiation into cells presenting neuronal-like morphologies within 24 hours of induction (4, 5, 7, 8). Consistent with these morphological changes, BME induced MSCs have been noted to express neuronal specific markers such as Neuron specific enolase (NSE), β-Tubulin 3 (βT3), Glial Fibral Acidic Protein (GFAP), S-100 and Neudesin (NENF) (4, 5, 7, 8).

However, determining the functionality of the produced cells has proved to be much more difficult. The function of BME transdifferentiated cells or the ability of the produced cells to conduct an action potential would prove the cells produced are terminally differentiated neurons. Barnabé et al. (7) conducted patch clamping to detect the Na^+ and K^+ currents to determine electrophysiological potential, revealing that the produced cells did not show evidence of Na^+ or K^+ currents nor the ability to fire action potentials.

The characterisation of differentiation by determining the presence of a small number of markers using antibodies in Western blot or immunofluorescence can result in a false impression of the extent of differentiation. By examining the proteome profiles, an unbiased comparative and quantitative measurement of the extent of biological change through the differentiation process can be performed. Thus the aim of this study is the examination of these cells at the proteome level to investigate the changes in protein abundance of differentiating ADSCs in the presence of beta-mercaptoethanol.

Experimental Procedures

Cell culture

This research was approved by the Macquarie University human research ethics committee (Ref #: 5201100385). The procedure described below is adapted from Bunnell et al. (11). Adult ADSCs were derived from abdominal lipoaspirates and subsequent steps were conducted under sterile conditions in a class II laminar flow hood (Clyde-Apac BH2000 series). Lipoaspirates were rinsed twice in Dulbecco's Modified Eagle's Medium (D-MEM, Gibco), connective tissue digested with collagenase type 1 (Gibco) for 45 minutes at 37°C before centrifugation at 1600×g for 10 minutes at 4°C to separate adipocytes from the stromal vascular fraction (SVF). The pellet was resuspended in 3 ml of D-MEM and layered on top of 3 ml of Ficoll Paque PLUS (Sigma-Aldrich) to remove red blood cells from the SVF. The resulting purified stromal vascular fraction (SVF) was aliquoted into a T25 culture flask (Nunc) in Delbucco's modified eagle medium (D-MEM) Glutmax/F12 (Gibco) with 10% Fetal bovine serum (FBS) (Invitrogen) and 1% antibiotics/antimycotics (ABAM) (Invitrogen) and incubated at 37°C at 5% CO_2 for 48 hours until ADSCs adhered to the culture flask. Non-adherent cells were eliminated by replacing the media. All isolations were confirmed CD45 negative and CD90 positive (data not shown). ADSCs were passaged 3～5 times by detaching cells with TrypLE Express (Gibco) and before being utilised in differentiation experiments.

Chemical induction for differentiation

Subconfluent ADSCs were washed twice in pre-warmed sterile D-MEM/F12 (Invitrogen). The cells were then cultured for a further 24 hours in a serum-free pre-induction medium consisting of D-MEM/F12 (Invitrogen), Antibiotics-Antimycotics (ABAM, Invitrogen) and 1 mM β-mercaptoethanol (Sigma). The media was then replaced after 24 hrs with the neural inducing media consisting of D-MEM/F12 (Invitrogen), ABAM (Invitrogen) and 10 mM β-mercaptoethanol (Sigma) as per Woodbury et al. (4).

Glioblastoma cell culture

GBCs line (NCH612 Cell Line Service, Germany) were cultured D-MEM/F12 (Invitrogen), ABAM (Invitrogen). The cells were grown to 90% confluence prior to passaging or harvesting for proteomics.

Microscopy

Cell counts

In vitro cell counts were carried out utilising a novel procedure to determine the approximate colony forming units per square millimetre of cells adherent to the culture flask which were induced for differentiation and subsequently utilised for proteomics. A grid of squares 2.5 ×2.5 mm was printed on a transparent laminate and cut to fit outer bottom side of a T175 culture flask (BD Falcon). Ten squares were chosen and cells counted at 100X on an Olympus CK40 inverted microscope and the cell counts from the ten squares were averaged for each flask to find a mean total cfu per square. For the flask total cell population, the averaged cell number was multiplied by 28000 (16squares*10*175 cm) to find the total cell population in the T175 culture flask. To find cfu/mm^2 the average cell number from the ten squares were divided by 2.5 mm. At the final time point cells were removed from the culture flask and an aliquot was stained with trypan blue to determine live/dead ratio using a Neubauer chamber. The total cell number data was also utilised in the Bioplex analysis (described below) to determine the amount of cytokines secreted per cell. This was calculated by multiplying the concentration by the total volume of the flask and dividing by the total cell number at the respective time point. Stained cells were visualised on an Olympus IX51 inverted microscope and images captured with the attached Olympus DP70 camera.

Protein Extraction

Culture media was decanted and the cells washed 2～3 times with sterile 1X Phosphate buffered saline (PBS). Cells were harvested by treating cells with 3 ml TrypLE Express (12604 Gibco) for 10～15 minutes at 37°C. Detached cells were rinsed and collected in 10 ml of sterile 1X PBS in a 15 ml falcon tube. Cells were centrifuged at 1000 rcf for 10 minutes to pellet. Supernatant was decanted and the cell pellet was resuspended in 100 μl of 1% SDS and transferred to 0.65 ml eppendorf tube and boiled for 10 minutes to lyse cell pellets. Lysates were centrifuged at 16000 rcf for 10 minutes to pellet debris. Supernatant was then buffer exchanged into 0.1% SDS with SCC Micro-Biospin columns (BioRad).

1D Electrophoresis

Samples were diluted 1:1 with SDS loading buffer (Invitrogen), heated at 95°C for 10 minutes then centrifuged. Samples were then loaded into 4～12% Bis-Tris Criterion gel (BioRad) in XT-MES (BioRad) running buffer then electrophoresed according to the standard product protocol of 160 V for 50 minutes (BioRad). Upon completion of electrophoresis, gels were either used in western blots or fixed and stained with Flamingo fluorescent protein stain (Biorad). Gels were imaged using a PharosFX Plus (Biorad) imager and Quantity One software (BioRad). The gel was then was over stained with Coomassie Blue G stain for visual comparison.

Western Blot

The Western blot method was adapted from Jobbins et al. (12). The membrane was then placed in a solution containing the one of the following primary monoclonal antibodies: mouse anti-human NeuN/Fox3 (M377100 Biosensis 1:5000), mouse anti-human NF200 (M988100 Biosensis 1:500), rabbit anti-human βT3 (ab18207 Abcam 1:1000) or rabbit anti-human GFAP (ab7260 Abcam 1:50000) diluted in PBS respectively and incubated overnight at 4°C on a gentle rocker. Subsequently washed 3 times with PBS and probed with a secondary antibody either and anti-mouse IgG (A4416 Sigma) or anti-rabbit IgG (A4312 Sigma) dependent on the primary probe. Secondary antibodies were peroxidase or alkaline phosphatase conjugated for development with 3, 3-Diaminobenzidine (DAB) (Sigma) or 5-bromo-4-chloro-3-indolyl phosphate/nitro blue tetrazolium chloride (BCIP/NBT) (Sigma) respectively.

Bioplex

ADSCs and differentiation conditioned media in 500 μl aliquots were collected at time 0min as a control and at 30 min, 1 hr, 3 hrs, 5 hrs, 20 hrs and 24 hrs subsequent to adding the differentiation media and then stored at −80 degC till assay. Concentrations of IL-1ra, IL-1b, IL-2, IL-4, IL-5, IL-6, IL-7, IL-8, IL-9, IL-10, IL-12 (p70), IL-13, IL-15, IL-17, Eotaxin, FGF basic, G-CSF, GM-CSF, IFN-γ, MCP-1, MIP-1a, MIP-1b, PDGF-bb, RANTES, TNF-α and vEGF were simultaneously evaluated using a commercially available multiplex bead-based sandwich immunoassay kits (Bioplex human 27-plex, M50-0KCAF0Y BioRad Laboratories). Assays were performed according to the manufacturer's instructions.

iTRAQ

After cell lysis and protein extraction the total of 4 samples for iTRAQ labelling (1～ ADSCs, 2～ 12 hr BME

Differentiation hADSC, 3～24 hr BME Differentiation hADSC and 4～ Glioblastoma control [GBCs]) were buffer exchanged in 0.1% SDS using a Tris free Micro Bio-Spin Chromatography Columns (BioRad) and made up to a final concentration of 60 μg/100 μl each. iTRAQ labelling was performed as per manufacturer's instructions. Following labelling, samples were combined and fractionated by strong-cation exchange (SCX) chromatography with Polysulfoethyl A column. The SCX fractions were injected with an Eksigent Ultra nanoLC system (Eksigent) onto a ProteCol C18 column (SGE) and peptides eluted using a linear gradient at 600 nl/min over 100 minutes. The eluent was subject to positive ion nanoelectrospray analysis in an information dependant acquisition mode (IDA) with a TripleTOF 5600 (AB Sciex). In IDA mode, a TOFMS survey scan was acquired (m/z 400～1,500, 0.25 second), with the ten most intense multiply charged ions (counts ＞150) in the survey scan sequentially subjected to MS/MS analysis. MS/MS spectra were accumulated for 200 milliseconds in the mass range m/z 100～1500 with the total cycle time 2.3 seconds. MS/MS data were submitted to ProteinPilot V4.0 (AB Sciex) for data processing using *Homo sapiens* species. Bias correction was selected. The detected protein threshold (unused ProtScore) was set as larger than 1.3 (better than 95% confidence). FDR (False discovery rate) Analysis was selected. A minimum of five peptide cut-off stringency was used to identify proteins. Volcano plots, Gene ontology and Bioplex heat maps were generated using DanteR software (13).

Results

Microscopy

Human ADSCs (hADSCs) were cultured producing a morphologically homogenous culture with cells exhibiting the spindle-fibroblastic form consistent with current literature. The cells were maintained at subconfluency prior to addition of differentiation media containing BME as per Woodbury et al. (4). Fig. 1A～D shows the rate of cellular remodelling over a 24 hour period after the addition of the differentiation media. Basal ADSCs (Fig. 1A) generally grow in a flat, large fibroblastic configuration. Within 3 hours (Fig. 1B) of neuronal induction the morphological changes became evident with a number of cells

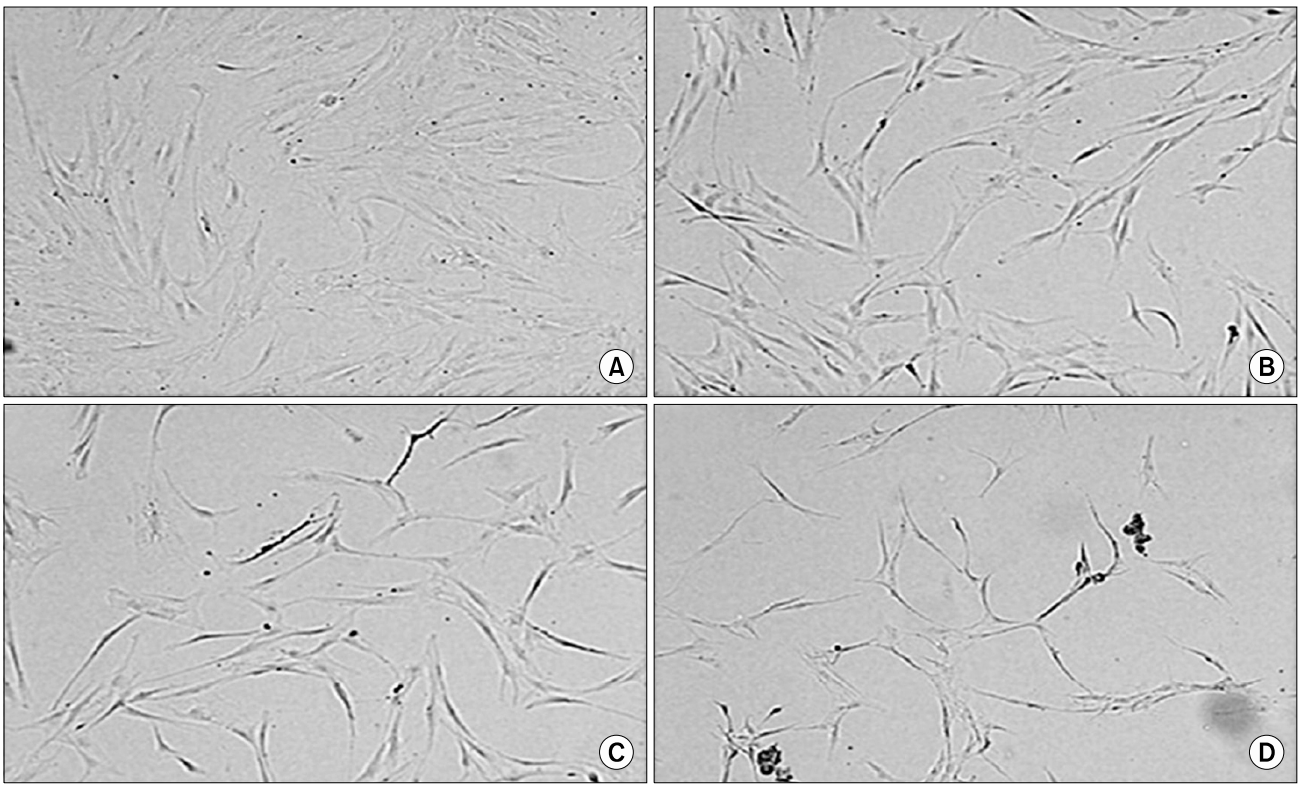

Fig. 1. Morphological comparisons between non-induced ADSCs and chemically induced ADSCs. (A) Basal human ADSCs cultured as a control prior to differentiation presents standard flat fibroblastic morphology. (B～D) hADSCs post induction 3 hours, 12 hours and 24 hours with neurodifferentiation media with the progressive structural remodelling over the 24 hour time period. 10×Magnification.

showing signs of cytoplasmic retraction toward the nucleus of the cell. The now elongated membrane produced a firm and contracted bipolar or multi-polar configuration. At the 12 hour time point (Fig. 1C) the cells morphological changes are ubiquitous across the cultured population with a majority of the cells presenting the retracted cytoplasm and multi-polar shape with evidence of extensions and processes reaching between cells. The cell bodies appear condensed and light refractive compared to the basal hADSCs. At the 24 hour time point prior to harvesting, the cells have a unique morphology compared to the basal state hADSCs with the majority of adherent cells producing polar extensions and processes reaching between cells with some evidence of detachment. In summary these cells morphologically appear to resemble neuronal cells.

iTRAQ proteome comparisons of hADSCs, 12 hour, 24 hour differentiated and GBCs control

The digested proteins from each cell line were labelled with the iTRAQ isobaric tags as follows: hADSCs, 12 hour differentiated hADSCs, 24 hour differentiated hADSCs and GBCs labelled with 114, 115, 116 and 117 isobaric tags respectively. The protein fold changes between samples were done comparatively and are relative to a base denominator, the basal hADSCs -114, and all comparisons were made relative to this, i.e. 115 vs 114, 116 vs 114 and 117 vs 114. This was done to elucidate the relative protein fold changes across the captured and labelled proteome of the differentiating cells, determining the up or down regulation of protein species over time during differentiation.

Table 1 summarises the iTRAQ results of basal hADSCs, hADSCs differentiated for 12 hours, hADSCs differentiated for 24 hours and a control GBCs cell line. The summary table shows the upper 99%, 95% and 66% cut off for detected proteins. The upper 95% range was chosen for all data analysis and, within that cutoff, a total of 2,568 proteins consisting 38,786 distinct peptides were identified from 171,862 spectra (Table 1). An average of 5.89 peptides was matched per protein with an average of 13.88% sequence coverage from the total cohort of the detected proteins. The total number of proteins identified by a single peptide match was 980 proteins from the 2,568 identified which is approximately 37% of identified proteins. The analysis cut off removed proteins with below the average peptides matched (i.e. 5 peptides/protein) to increase the robustness of the dataset and the conclusions drawn. A table of all of the above proteins is available in supplementary material 1A. The subsequent cut offs utilised were based on p-value (<0.05) and fold change ($\log_2 < -0.2$ or $0.2 >$). These partitions refine the later analyses to statistically significant proteins which have an average of 20 matched peptides per protein. The ProteinPilot group file, the protein summaries and peptide summary (without background corrections) were exported to XML format for further analysis with specified denominators for inter-sample comparisons through the generation of volcano plots and gene ontology graphs.

Volcano plots were generated to visualise the up/down regulated proteins, showing p-values versus the $\log_2$ protein fold change of each experimental cell line vs. Basal hADSCs of all 2,568 proteins. The quantitation criteria cut off of significant protein fold changes were completed statistically with the students t-test at p-values of <0.05 and $\log_2$ fold change cut off of -0.2 or >0.2. This found 2,418 proteins were directly comparable between any two sample types at a time (Fig. 2A~C). The blue nodes outside the horizontal and vertical asymptotes represent the statistically significant changed proteins above >0.2 log fold change up-regulated proteins and the below <0.2 fold change down-regulated proteins. The grey nodes represent the non-significantly changed proteins with a p-value $>$ 0.05 and within the cut off for fold change.

The number of statistically significant up and down regulated proteins from each fold comparisons between 12 hr differentiated vs ADSCs (115v114) revealed 81 up regulated and 171 down regulated (Fig. 2A) proteins, comparisons between 24 hr differentiated vs ADSCs (116v114) revealed 85 up regulated and 138 down regulated proteins (Fig. 2B), and comparisons between GBCs vs ADSCs (117v114) revealed 429 up regulated and 504 down regulated proteins (Fig. 2C).

Fig. 2D exhibits the ratio of statistically changed pro-

Table 1. Mass spectrometry iTRAQ protein and peptides counts with relative cutoffs of ADSCs, ADSCs differentiated for 12 hours and 24 hours and glioblastoma cells protein pilot results

Confidence cutoff	Proteins detected	Proteins before grouping	Distinct peptides	Spectra identified	% total spectra
>2.0 (99)	2203	2948	37370	169630	66.8
>1.3 (95)	2568	3505	38786	171862	67.7
>0.47 (66)	2886	5410	40209	173935	68.5
Cutoff applied: >0.05 (10%)	3760	16315	43347	178197	70.2

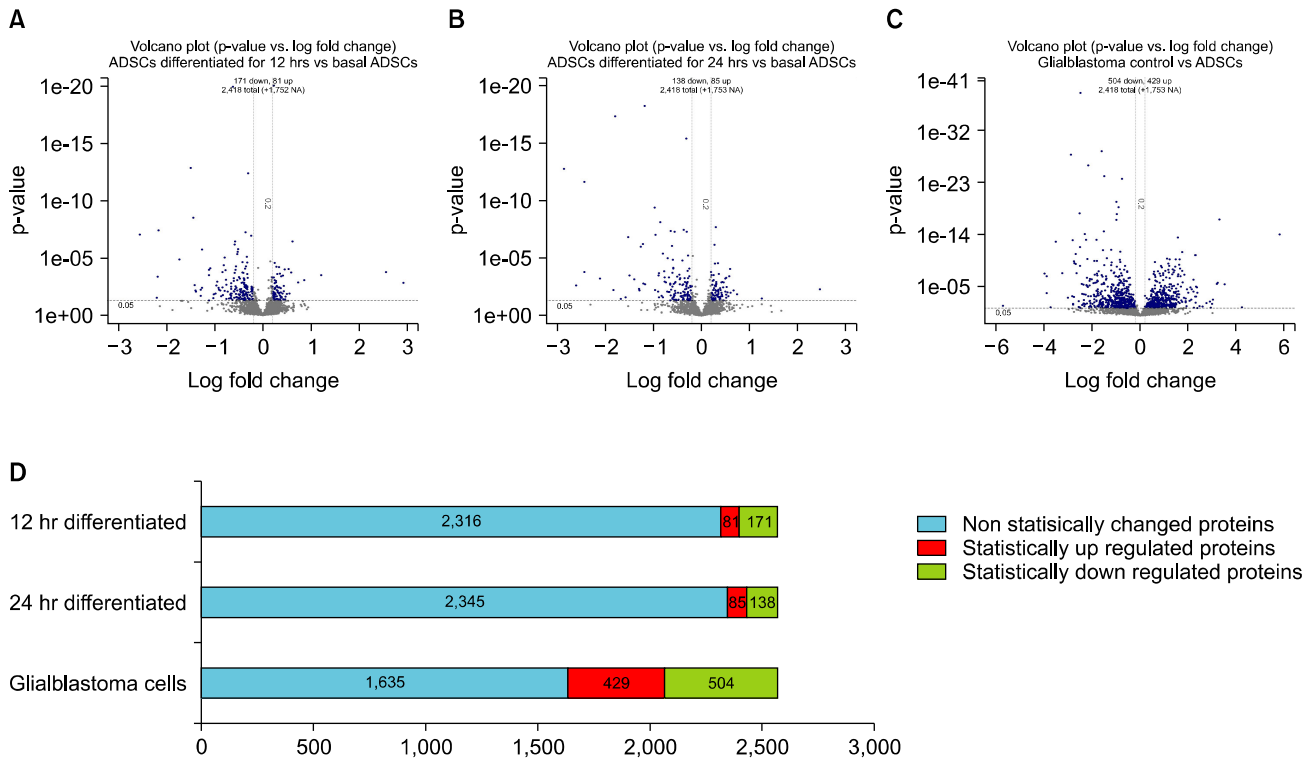

Fig. 2. Volcano plots. (A∼C) showing p-values versus protein fold change (log_2) of ADSCs and comparisons. Quantitation criteria cutoff of statistically significant p-values <0.05 and log_2fold change cutoff of <−0.2 or >0.2. The blue nodes represent the above >0 log fold change i.e. up-regulated proteins and the below <0 fold change down-regulated proteins. The grey nodes represent the not significantly changed proteins with a p-value >0.05 and within the cut off for fold change. D shows the ratio of statistically changed proteins across all samples compared to basal ADSCs. Blue bar presents non-statistically significant changed proteins, red bar is the statistically significant up regulated proteins and green is the statistically significant down regulated proteins.

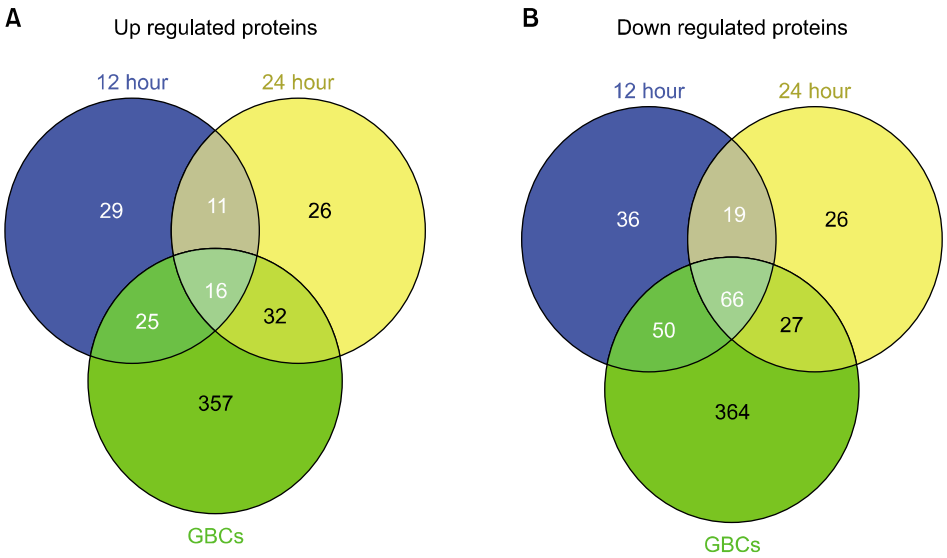

Fig. 3. Three-way Venn diagrams of up and down regulated proteins. Diagrams include the 12 hour differentiated, 24 hour differentiated hADSCs and the GBCs showing unique and shared proteins. (A) shows up regulated proteins revealing there are 29, 26, 357 unique proteins with 11, 32 and 25 shared proteins between each of the corresponding tested cell lines as well as 16 shared proteins between all three relative to basal hADSCs. (B) shows down regulated proteins revealing there are 36, 26, 364 unique proteins with 19, 27 and 50 shared proteins between each of the corresponding tested cell lines as well as 66 shared proteins between all three relative to basal hADSCs.

teins across all samples compared to basal ADSCs in the form of a bar graph. The blue bar presents non-statistically significant changed proteins, red bar is the statistically significant up regulated proteins and green is the statistically significant down regulated proteins.

The Venn diagrams in Fig. 3 presents the statistically relevant up/down regulated proteins that are unique and shared between each time point and the control cell line. Table 2A and 2B presents the *up* and *down* regulated proteins respectively. The data listed shows the unique and common proteins to each differentiation time point and their statistical significance as well as fold change relative to the ADSCs. Furthermore the table also shows the relative fold change and p-value of proteins in the other time points to present the extent of change in expression of proteins between the time points. Table 2C presents important proteins related to neurogenesis by cell proliferation, cell differentiation, morphogenesis, cytoskeleton remodelling or response to stress or shock by function according to Gene Ontology biological processes. The mutual expression of neurogenic and stress related proteins indicates the cells are experiencing a directed push toward a phenotype expressing neuronal proteins however the stress proteins indicate that the chemical differentiation is traumatic to the cells and is damaging them throughout the process.

The down regulation of significant numbers and types of cytoskeletal related proteins, such as actin and tubulin proteins, in the 12 and 24 hr differentiated ADSCs to levels consistent with the GBCs indicates a large morphological restructuring of the cell as identified during microscopy, or damage. The relatively large decrease in myosin related proteins in both differentiation time points indicates that the differentiating cells have shifted away from a mesodermal lineage. This trend is further supported by the mass down regulation of pro-collagen and collagen related structural proteins which, when in high abundance, play a pivotal role in connective tissue, adipose, cartilage and bone formation. Conversely a down regulation of similar structural support proteins is also an indication of cellular damage and stress which has been noted to occur in acute epithelial cell injury (14), and this is covered further in the discussion.

A decrease in the enzyme alpha enolase and the relative increase in gamma enolase/NSE levels are consistent with the development of neuronal tissue seen in rats and humans (15). A switch from alpha enolase, which is mesodermal specific, to gamma enolase which is ectodermal/neuronal specific is often used as an enzymatic biomarker for neuronal development (16). The levels of alpha enolase detected in the differentiation time points are equivalent to the GBC cell line. However, the detected levels of up regulated NSE within the differentiated and GBCs lies in the non-statistically significant identified proteins.

Western Blots

The majority of the aforementioned proteins have more than 5 unique positively matched peptides (Supplementary Table 1). This larger list of neuronal related proteins were deemed to be important and required further investigation as three out of the four most widely used markers for neurogenic differentiation (4-6), Neuron specific enolase (NSE), Neudesin (NENF) and Beta-tubulin III (βT3) fell within this statistically non-significant, up regulated neuronal related protein cut off group. The fulfillment of the 5 peptides or greater cut-off suggests that these molecules are changing but not statistically significantly. Western blots to detect the commonly used neuronal markers βT3, GFAP, NF200 and NeuN were carried out to compare these protein's expression in the BME treated ADSCs with GBC whole cell lysates in this study and previous literature. βT3 is a 55 kDa protein which is positively detected in the basal ADSCs, the BME differentiated ADSCs and the GBCs (Fig. 4A). The GFAP molecule is only detected at the 48 kDa mark in the GBC lane at a normal exposure (Fig. 4B). By decreasing the contrast by 20%, the GFAP is just detectable in the BME differentiated cells. The NF200 protein is detected in both the ADSC differentiated and with a slightly stronger presence in the GBC at 200 kDa while there is no trace present in the BME lane (Fig. 4C). The NeuN however was not detected in the ADSCs but very faintly in the BME differentiated and GBCs (Fig. 4D). βT3 has been used to characterise primitive neuroepithelium and catalogued as being solely expressed on neuronal cells (17) however βT3 has been found to be expressed in the ADSCs within this study. Similarly the presence of NeuN in the ADSCs confounds the use of this protein as a neuronal specific marker. Thus the identification and quantitatation of the extent of differentiation with relatively few markers is insufficient thus supporting the wider proteomic analysis.

Cell Counts

The total cell count and average cfu/mm^2 trends (Fig. 5) are identical presenting no change in cell population in the triplicate flasks from basal cells up to 1 hr post induction. The basal population counts averaged at 77

Table 2A. Up regulated proteins identified in Volcano plots with fold change and p-values relative to ADSCs. The table also includes the data for the same protein in all other samples showing its relative fold change and p-value in that respective sample

Accession and gene name	Protein name	12 hr:ADSC fold change	12 hr:ADSC p-value	24 hr:ADSC fold change	24 hr:ADSC p-value	GBC:ADSC fold change	GBC:ADSC p-value
Proteins only in 12 hr differentiation							
sp|Q09666|AHNK_HUMAN	Neuroblast differentiation-associated protein AHNAK	1.172291994	9.64E-21	0.932504714	0.0007391	0.284376711	0
sp|Q14697|GANAB_HUMAN	Neutral alpha-glucosidase AB	1.166213036	0.000511139	1.070240021	0.222811505	0.589860618	9.70205E-08
sp|O94979|SC31A_HUMAN	Protein transport protein Sec31A	1.163427949	0.008623381	0.957205117	0.283038706	0.492330998	1.42785E-07
sp|P34897|GLYM_HUMAN	Serine hydroxymethyltransferase, mitochondrial	1.229635	0.000259559	1.008682966	0.852325201	0.86065948	0.003069297
sp|O94925|GLSK_HUMAN	Glutaminase kidney isoform, mitochondrial	1.167204976	0.023215359	0.888292372	0.245319307	0.611154675	0.00079499
sp|Q92616|GCN1L_HUMAN	Translational activator GCN1	1.223534942	0.03858383	1.014554024	0.78253752	0.767004311	0.036446411
sp|P37837|TALDO_HUMAN	Transaldolase	1.221547961	0.002808012	1.07517004	0.231923506	0.985290229	0.7554124
sp|P16152|CBR1_HUMAN	Carbonyl reductase (NADPH) 1	1.174060941	0.026851811	1.127655983	0.075313449	0.43443799	7.23315E-05
sp|Q3SY69|AL1L2_HUMAN	Mitochondrial 10-formyltetra-hydrofolate dehydrogenase	1.198042989	0.024666181	0.933903277	0.495610595	0.220972598	1.12357E-05
sp|P16070|CD44_HUMAN	CD44 antigen	1.291394949	0.00441253	1.032801032	0.627236784	0.547489822	0.01207258
sp|Q15063|POSTN_HUMAN	Periostin	1.500138998	0.000187826	0.58855629	0.001084263	0.342270195	0.004329615
sp|Q16666|IF16_HUMAN	Gamma-interferon-inducible protein 16	1.171751976	0.046327461	1.145359039	0.042793728	0.541573286	0.00104327
sp|Q12797|ASPH_HUMAN	Aspartyl/asparaginyl beta-hydroxylase	1.243144989	0.003729993	1.005350947	0.936527789	0.712441385	0.01231128
sp|O14980|XPO1_HUMAN	Exportin-1	1.200220942	0.01458496	1.043936968	0.47226429	0.972239017	0.733839929
sp|O94855|SC24D_HUMAN	Protein transport protein Sec24D	1.188967943	0.044853151	1.013072968	0.830020487	0.428946793	0.00079677
sp|O75533|SF3B1_HUMAN	Splicing factor 3B subunit 1	1.294285059	0.02979246	1.095713019	0.31003201	0.924929082	0.493676394
sp|P12111|CO6A3_HUMAN	Collagen alpha-3 (VI) chain	1.334668994	0.000342844	0.809870183	0.001698597	0.383068711	0.001706147
sp|P09601|HMOX1_HUMAN	Heme oxygenase 1	2.30873394	0.000330115	1.018610001	0.799727917	0.435669094	0.00274237
sp|Q15459|SF3A1_HUMAN	Splicing factor 3A subunit 1	1.221204996	0.006248812	1.127351999	0.107962303	1.206622005	0.062194299
sp|P09619|PGFRB_HUMAN	Platelet-derived growth factor receptor beta	1.190086007	0.04670446	0.741432011	0.05704977	0.264767289	0.019523449
sp|Q92841|DDX17_HUMAN	Probable ATP-dependent RNA helicase DDX17	1.218611002	0.02252163	1.04066503	0.538156688	1.076015949	0.290756613
sp|Q04828|AK1C1_HUMAN	Aldo-keto reductase family 1 member C1	1.809262037	0.000905988	1.438812017	0.084717967	0.991984606	0.936510086
sp|Q5SSJ5|HP1B3_HUMAN	Heterochromatin protein 1-binding protein 3	1.41080296	0.01353518	1.191717982	0.150823593	0.80679673	0.250696898
sp|Q9BUJ2|HNRL1_HUMAN	Heterogeneous nuclear ribonucleoprotein U-like protein 1 1	1.237962961	0.007558046	1.13301301	0.144437	0.719004393	0.034528211
sp|P55263|ADK_HUMAN	Adenosine kinase	1.199633002	0.04212771	1.184255958	0.118330203	0.716779828	0.024615809
sp|A1X283|SPD2B_HUMAN	SH3 and PX domain-containing protein 2B B	1.273609042	0.01867228	1.111310959	0.169878498	0.939716518	0.643383682
sp|Q14914|PTGR1_HUMAN	Prostaglandin reductase 1	1.272560954	0.042743411	0.916326702	0.475612402	0.336828709	0.016600359

Table 2A. Continued

Accession and gene name	Protein name	12 hr:ADSC fold change	12 hr:ADSC p-value	24 hr:ADSC fold change	24 hr:ADSC p-value	GBC:ADSC fold change	GBC:ADSC p-value
sp|P50281|MMP14_HUMAN	Matrix metalloproteinase-14	1.339097023	0.0413494	1.198922038	0.1013465	0.805615783	0.137749895
sp|P49792|RBP2_HUMAN	E3 SUMO-protein ligase RanBP2	1.35255003	0.00835917	1.088907003	0.396347314	1.158911943	0.221689299
Common proteins in 12 and 24 hour differentiation							
sp|P08670|VIME_HUMAN	Vimentin	1.261533022	6.51117E-05	1.212504029	2.87636E-05	0.209194794	6.95276E-14
sp|P13010|XRCC5_HUMAN	X-ray repair cross-complementing protein 5	1.149952054	0.000521866	1.235864997	0.001566513	1.062132001	0.196620807
sp|P78527|PRKDC_HUMAN	DNA-dependent protein kinase catalytic subunit	1.185911059	2.83388E-05	1.204792023	6.77829E-07	1.086081028	0.068069547
sp|P19367|HXK1_HUMAN	Hexokinase-1	1.148920059	0.003355148	1.176377058	0.000913902	0.373809695	1.47925E-07
sp|P04181|OAT_HUMAN	Ornithine aminotransferase, mitochondrial	1.297075987	0.000400532	1.229442954	0.00214691	0.799335778	0.036058169
sp|Q9NVI7|ATD3A_HUMAN	ATPase family AAA domain-containing protein 3A	1.382269979	0.024106581	1.344267964	0.046113499	0.76491338	0.144031405
sp|Q13740|CD166_HUMAN	CD166 antigen	1.292449951	0.01025022	1.413301945	0.000594783	1.002328038	0.9778862
sp|Q1KMD3|HNRL2_HUMAN	Heterogeneous nuclear ribonucleoprotein U-like protein 2 2	1.163431048	0.025791969	1.162364006	0.037656728	0.687537313	0.01868871
sp|P22307|NLTP_HUMAN	Non-specific lipid-transfer protein	1.181208014	0.01080329	1.506800056	8.88028E-05	0.817267299	0.067778051
sp|P02792|FRIL_HUMAN	Ferritin light chain	5.841430187	0.000173394	1.289484024	0.02308102	1.064864993	0.623959184
sp|P08670|VIME_HUMAN	Vimentin	1.261533022	6.51117E-05	1.212504029	2.87636E-05	0.209194794	6.95276E-14
Proteins only in 24 hour differentiation							
sp|P11021|GRP78_HUMAN	78 kDa glucose-regulated protein	0.978915572	0.732581973	1.225558043	2.06624E-08	0.465184987	4.34353E-08
sp|P02545|LMNA_HUMAN	Prelamin-A/C	1.145071983	0.000569356	1.150127053	0.000163541	0.553177416	8.95206E-09
sp|Q01813|K6PP_HUMAN	6-phosphofructokinase type C	0.99266398	0.857660413	1.157106042	0.021628169	0.378134012	3.5279E-07
sp|P11940|PABP1_HUMAN	Polyadenylate-binding protein 1	1.006376028	0.935915887	1.172831059	0.01407769	0.810070574	0.001010054
sp|P19338|NUCL_HUMAN	Nucleolin	1.126765013	0.002805512	1.193856001	0.000299175	0.817295194	0.000231495
sp|O60701|UGDH_HUMAN	UDP-glucose 6-dehydrogenase	0.956641316	0.319954991	1.163594007	0.01503478	0.268783987	7.86066E-08
sp|Q8NBS9|TXND5_HUMAN	Thioredoxin domain-containing protein 5	0.985793471	0.751312375	1.218961954	0.006199135	0.547286689	1.33254E-07
sp|P14314|GLU2B_HUMAN	Glucosidase 2 subunit beta	1.07150197	0.201880306	1.230283976	0.002728704	0.787490726	0.00148304
sp|P26640|SYVC_HUMAN	Valine–tRNA ligase	1.060871005	0.1173729	1.149708986	0.01608438	1.007483959	0.905321598
sp|P62249|RS16_HUMAN	40S ribosomal protein S16	0.858236015	0.004291136	1.211066008	0.00240164	0.712900877	1.01167E-05
sp|P61019|RAB2A_HUMAN	Ras-related protein Rab-2A	1.065119028	0.217482507	1.162690043	0.01066714	1.080078006	0.288548201
sp|P62750|RL23A_HUMAN	60S ribosomal protein L23a	0.693098485	0.00086417	1.189059019	0.01703758	0.487416297	0.000572545
sp|Q00325|MPCP_HUMAN	Phosphate carrier protein, mitochondrial	1.101160049	0.277084112	1.285720944	0.000241725	0.833141625	0.028220629
sp|P42765|THIM_HUMAN	3-ketoacyl-CoA thiolase, mitochondrial	1.173899055	0.053517099	1.234925032	0.001965876	0.3427625	0.000915591
sp|P23219|PGH1_HUMAN	Prostaglandin G/H synthase 1	1.103464961	0.151414096	1.216788054	0.002485003	0.239393905	0.000434135
sp|P50402|EMD_HUMAN	Emerin	0.998557806	0.981318891	1.194576025	0.030741731	0.989170074	0.857835472

Table 2A. Continued

Accession and gene name	Protein name	12 hr:ADSC fold change	12 hr:ADSC p-value	24 hr:ADSC fold change	24 hr:ADSC p-value	GBC:ADSC fold change	GBC:ADSC p-value
sp|P31942|HNRH3_HUMAN	Heterogeneous nuclear ribonucleoprotein H3	1.038696051	0.730665028	1.252938032	0.015092	1.122933984	0.502929688
sp|P51572|BAP31_HUMAN	B-cell receptor-associated protein 31	0.848266423	0.139359504	1.263605952	0.01813079	0.578480422	9.32726E-05
sp|P24534|EF1B_HUMAN	Elongation factor 1-beta	1.026842952	0.733575523	1.209748983	0.01879742	0.708731711	0.023696421
sp|P62851|RS25_HUMAN	40S ribosomal protein S25	0.752057493	0.02106422	1.257261992	0.021622639	0.640693009	0.028522549
sp|P13645|K1C10_HUMAN	Keratin, type I cytoskeletal 10	1.020138025	0.882443428	1.468924046	0.020549349	1.615792036	0.058578409
sp|P02768|ALBU_HUMAN	Serum albumin	0.607474923	0.083786011	5.504323006	0.005226725	0.730836689	0.622102082
sp|Q00765|REEP5_HUMAN	Receptor expression-enhancing protein 5	0.790062189	0.2131235	1.426352024	0.02796719	0.362138212	0.040924039
sp|Q6PIU2|NCEH1_HUMAN	Neutral cholesterol ester hydrolase 1	0.933943689	0.603259921	1.301720977	0.037261799	1.251042962	0.191826195
sp|Q15382|RHEB_HUMAN	GTP-binding protein Rheb	1.032513022	0.62273711	1.22151804	0.032001801	1.228466988	0.154868901
sp|P02765|FETUA_HUMAN	Alpha-2-HS-glycoprotein	1.116534948	0.785439074	2.379687071	0.031562109	0.457956403	0.071328543
Common proteins in 24 hour differetiation and GBCs							
sp|P38646|GRP75_HUMAN	Stress-70 protein, mitochondrial	1.117077947	0.003131488	1.152879	0.000309053	1.659019947	2.0803E-08
sp|P06576|ATPB_HUMAN	ATP synthase subunit beta, mitochondrial	1.134068012	0.01257757	1.243697047	0.006840608	1.523617983	8.35058E-08
sp|P21796|VDAC1_HUMAN	Voltage-dependent anion-selective channel protein 1	1.003872991	0.95314759	1.222074032	0.01048861	1.796416044	1.28039E-07
sp|Q15233|NONO_HUMAN	Non-POU domain-containing octamer-binding protein	1.090173006	0.390620798	1.158053041	0.025060721	1.585235	0.00078185
sp|P05141|ADT2_HUMAN	ADP/ATP translocase 2 SV=7	1.099650025	0.238759294	1.379487991	0.046200089	2.126817942	0.003026843
sp|Q06830|PRDX1_HUMAN	Peroxiredoxin-1	0.871106803	0.264881313	1.368083	0.003427934	3.878715038	2.48676E-05
sp|P29692|EF1D_HUMAN	Elongation factor 1-delta	0.885660887	0.295335889	1.219599009	0.018010911	1.424182057	0.001063915
sp|P16401|H15_HUMAN	Histone H1.5 B	1.139510036	0.467794806	1.377078056	0.001285438	2.052494049	0.000144169
sp|P45880|VDAC2_HUMAN	Voltage-dependent anion-selective channel protein 2	1.132365942	0.02972977	1.490978956	0.000377296	1.414775014	2.3224E-05
sp|P07910|HNRPC_HUMAN	Heterogeneous nuclear ribonucleoproteins C1/C2	0.971731186	0.717681229	1.286700964	0.02625324	2.433696985	3.47498E-06
sp|P62807|H2B1C_HUMAN	Histone H2B type 1-C/E/F/G/I BC	1.22874105	0.1967251	1.67374599	0.01449305	2.993794918	0.004183407
sp|P09429|HMGB1_HUMAN	High mobility group protein B1	0.988982081	0.881807089	1.202600002	0.04294645	3.086293936	0.000200443
sp|Q07955|SRSF1_HUMAN	Serine/arginine-rich splicing factor 1	1.095106959	0.265865386	1.201938987	0.00424019	1.768741965	3.07727E-05
sp|P04264|K2C1_HUMAN	Keratin, type II cytoskeletal 1	1.165982008	0.078902021	1.277953982	0.01247019	1.712561965	8.00445E-05
sp|P61604|CH10_HUMAN	10 kDa heat shock protein, mitochondrial	1.032845974	0.786881626	1.425225973	0.000507918	4.02592802	0.000107939
sp|P54819|KAD2_HUMAN	Adenylate kinase 2, mitochondrial	1.184010983	0.089830346	1.159695983	0.0410228	2.850018024	0.000481253
sp|P48047|ATPO_HUMAN	ATP synthase subunit O, mitochondrial	1.206140041	0.121099599	1.240339994	0.007240169	2.975781918	3.41347E-06
sp|P30040|ERP29_HUMAN	Endoplasmic reticulum resident protein 29	1.132840991	0.089152887	1.304239988	0.004158478	1.905606031	4.23384E-05
sp|P55809|SCOT1_HUMAN	Succinyl-CoA:3-ketoacid-coenzyme A transferase 1, mitochondrial	1.08603096	0.384135008	1.168838024	0.03560289	1.913094044	7.59599E-05

Table 2A. Continued

Accession and gene name	Protein name	12 hr:ADSC fold change	12 hr:ADSC p-value	24 hr:ADSC fold change	24 hr:ADSC p-value	GBC:ADSC fold change	GBC:ADSC p-value
sp|P30048|PRDX3_HUMAN	Thioredoxin-dependent peroxide reductase, mitochondrial	1.140601039	0.205778703	1.308897972	0.03252491	1.476688981	0.01063342
sp|O43615|TIM44_HUMAN	Mitochondrial import inner membrane translocase subunit TIM44	1.260874987	0.149317995	1.35213697	0.019851711	1.588986993	0.02601867
sp|P20674|COX5A_HUMAN	Cytochrome c oxidase subunit 5A, mitochondrial	0.955496788	0.532972097	1.432423949	0.003153357	2.307585001	0.001240918
sp|P62316|SMD2_HUMAN	Small nuclear ribonucleoprotein Sm D2	1.098526955	0.202832907	1.186823964	0.042421039	1.349547982	0.003658696
sp|P53999|TCP4_HUMAN	Activated RNA polymerase II transcriptional coactivator p15	1.086330056	0.211981803	1.267210007	0.007258907	1.488083959	0.000537378
sp|P10606|COX5B_HUMAN	Cytochrome c oxidase subunit 5B, mitochondrial	0.848554611	0.121159598	1.343062997	0.01480979	1.891677976	0.000901474
sp|O75964|ATP5L_HUMAN	ATP synthase subunit g, mitochondrial	1.172261953	0.187723204	1.40666604	0.00825082	1.656165004	0.035087962
sp|O96000|NDUBA_HUMAN	NADH dehydrogenase (ubiquinone) 1 beta subcomplex subunit 10	1.11245501	0.230981693	1.319332004	0.006097732	1.663108945	0.00063837
sp|P13073|COX41_HUMAN	Cytochrome c oxidase subunit 4 isoform 1, mitochondrial	0.888194323	0.194232598	1.313930035	0.022194089	1.592439055	0.007572151
sp|Q13217|DNJC3_HUMAN	DnaJ homolog subfamily C member 3	1.233855009	0.054494139	1.153900981	0.02561407	1.394314051	0.007471726
sp|Q04837|SSBP_HUMAN	Single-stranded DNA-binding protein, mitochondrial	1.137815952	0.129254803	1.335986972	0.01021253	2.894625902	0.000223126
sp|Q00059|TFAM_HUMAN	Transcription factor A, mitochondrial	1.092440963	0.254071087	1.199000001	0.044862211	2.639131069	0.001804102
sp|P56385|ATP5I_HUMAN	ATP synthase subunit e, mitochondrial	1.176403046	0.162036195	1.521949053	0.01031177	1.912840009	0.025020519
Common proteins in 12 hour differentation and GBCs							
sp|P14136|GFAP_HUMAN	Glial fibrillary acidic protein	1.154310942	0.0131898	0.740810096	0.149216503	55.9920311	7.59313E-15
sp|Q14195|DPYL3_HUMAN	Dihydropyrimidinase-related protein 3	1.191656947	0.004737561	0.828772426	0.064621016	9.392551422	1.8213E-06
sp|P42330|AK1C3_HUMAN	Aldo-keto reductase family 1 member C3	1.375355959	0.040721409	0.903520823	0.652826726	6.757525921	0.00714481
sp|P48735|IDHP_HUMAN	Isocitrate dehydrogenase (NADP), mitochondrial	1.187353969	0.001626035	0.76078701	0.00222761	4.958202839	3.07282E-11
sp|P55084|ECHB_HUMAN	Trifunctional enzyme subunit beta, mitochondrial	1.207440972	0.001359062	1.120684028	0.02199926	1.546249032	1.85189E-07
sp|P40939|ECHA_HUMAN	Trifunctional enzyme subunit alpha, mitochondrial	1.204138994	0.001025685	1.099599004	0.051374801	1.216922045	0.01704336
sp|O75367|H2AY_HUMAN	Core histone macro-H2A.1	1.193729997	0.001547737	1.19423902	0.081774823	1.935490012	9.13986E-08
sp|P30084|ECHM_HUMAN	Enoyl-CoA hydratase, mitochondrial	1.19718504	0.003888754	1.14707005	0.01678746	4.252980232	1.23704E-05
sp|P49591|SYSC_HUMAN	Serine–tRNA ligase, cytoplasmic	1.19313395	0.01292462	1.044499993	0.504122615	1.816532969	0.000177273
sp|P62805|H4_HUMAN	Histone H4 A	1.447788954	9.72893E-05	1.521674991	0.103913099	2.227722883	0.000899077
sp|P15559|NQO1_HUMAN	NAD(P)H dehydrogenase (quinone) 1	1.654013991	0.00139986	1.019608974	0.757680178	4.643708229	6.49148E-05

Table 2A. Continued

Accession and gene name	Protein name	12 hr:ADSC fold change	12 hr:ADSC p-value	24 hr:ADSC fold change	24 hr:ADSC p-value	GBC:ADSC fold change	GBC:ADSC p-value
sp|O75874|IDHC_HUMAN	Isocitrate dehydrogenase (NADP) cytoplasmic	1.352331042	0.00269673	1.102399945	0.219124898	1.19700098	0.049357109
sp|O43809|CPSF5_HUMAN	Cleavage and polyadenylation specificity factor subunit 5	1.172230959	0.01696296	1.033825994	0.658303916	2.618022919	2.83626E-08
sp|P11177|ODPB_HUMAN	Pyruvate dehydrogenase E1 component subunit beta, mitochondrial	1.233819962	0.01056923	0.966665089	0.842215717	2.422485113	0.005875809
sp|P15121|ALDR_HUMAN	Aldose reductase	1.183169007	0.00527544	1.035091996	0.612842917	1.323901057	0.01107216
sp|P38159|RBMX_HUMAN	RNA-binding motif protein, X chromosome	1.345155954	0.042986959	1.251651049	0.063034117	1.742982984	0.006319256
sp|P09661|RU2A_HUMAN	U2 small nuclear ribonucleoprotein A'	1.172026038	0.032899201	1.122534037	0.093666807	1.966122031	4.43474E-05
sp|Q9UIJ7|KAD3_HUMAN	GTP:AMP phosphotransferase, mitochondrial	1.256214976	0.01342342	1.111209989	0.292258114	4.440637112	2.46386E-05
sp|Q9Y6C9|MTCH2_HUMAN	Mitochondrial carrier homolog 2	1.286370039	0.019908341	1.181535006	0.075119518	1.632563949	0.017359991
sp|P48507|GSH0_HUMAN	Glutamate–cysteine ligase regulatory subunit	1.466933012	0.01285504	1.085124016	0.338502586	2.536576986	0.001289886
sp|Q9Y305|ACOT9_HUMAN	Acyl-coenzyme A thioesterase 9, mitochondrial	1.322482944	0.01266097	1.062927008	0.345445514	1.47371304	0.007995555
sp|Q9BTT0|AN32E_HUMAN	Acidic leucine-rich nuclear phosphoprotein 32 family member E	1.24672699	0.044491019	1.267207026	0.108090602	2.464971066	0.000903143
sp|P07602|SAP_HUMAN	Proactivator polypeptide	1.230489016	0.037838642	0.899001718	0.459446788	1.434967995	0.033458289
sp|Q2M2I8|AAK1_HUMAN	AP2-associated protein kinase 1	1.262622952	0.040270969	1.039280057	0.582784116	1.330309987	0.03768494
Common proteins in 12, 24 hour differenttiation and GBCs							
sp|P25705|ATPA_HUMAN	ATP synthase subunit alpha, mitochondrial	1.212985992	6.15987E-05	1.237419963	0.00120072	2.068662882	1.71718E-08
sp|P40926|MDHM_HUMAN	Malate dehydrogenase, mitochondrial	1.186197996	0.000878019	1.269695044	2.80119E-05	4.914778233	2.84338E-11
sp|P34897|GLYM_HUMAN	Serine hydroxymethyltransferase, mitochondrial	1.153064013	0.01843836	1.189286947	0.000843555	2.34732604	1.77116E-10
sp|P00505|AATM_HUMAN	Aspartate aminotransferase, mitochondrial	1.265887022	0.003681256	1.250339031	0.007035483	2.955732107	1.33896E-07
sp|P49748|ACADV_HUMAN	Very long-chain specific acyl-CoA dehydrogenase, mitochondrial	1.369271994	0.000101588	1.352480054	0.001201282	2.553483009	9.20537E-09
sp|Q99623|PHB2_HUMAN	Prohibitin-2	1.274808049	0.000238774	1.183202028	0.006019574	1.941812992	4.42825E-08
sp|P52209|6PGD_HUMAN	6-phosphogluconate dehydrogenase, decarboxylating	1.526257992	3.7424E-07	1.167547941	0.002043512	2.10424304	2.09408E-07
sp|P35232|PHB_HUMAN	Prohibitin	1.191486955	0.004139135	1.277704954	0.008911012	1.738945007	6.2488E-05
sp|P36542|ATPG_HUMAN	ATP synthase subunit gamma, mitochondrial	1.270177007	0.01071905	1.335778952	0.001259367	2.829787016	6.42483E-05
sp|O75947|ATP5H_HUMAN	ATP synthase subunit d, mitochondrial	1.186648011	0.022031561	1.219419003	0.038824949	2.760775089	0.00011906

Table 2A. Continued

Accession and gene name	Protein name	12 hr:ADSC fold change	12 hr:ADSC p-value	24 hr:ADSC fold change	24 hr:ADSC p-value	GBC:ADSC fold change	GBC:ADSC p-value
sp|O43143|DHX15_HUMAN	Putative pre-mRNA-splicing factor ATP-dependent RNA helicase DHX15	1.159325957	0.028922981	1.17344296	0.047152009	1.422291994	0.016296981
sp|Q9Y277|VDAC3_HUMAN	Voltage-dependent anion-selective channel protein 3	1.309744	0.030049499	1.277943015	0.005669186	2.399842024	0.001137988
sp|P24539|AT5F1_HUMAN	ATP synthase subunit b, mitochondrial	1.309216022	0.024907401	1.586917996	0.006641487	2.33684206	0.00240706
sp|P02794|FRIH_HUMAN	Ferritin heavy chain	7.522081852	0.001523973	1.458412051	0.009750149	2.796227932	0.007973121
sp|Q07021|C1QBP_HUMAN	Complement component 1 Q subcomponent-binding protein, mitochondrial	1.285483003	0.046722271	1.427425027	0.01492106	4.938847065	0.006008915
sp|P14678|RSMB_HUMAN	Small nuclear ribonucleoprotein-associated proteins B and B'	1.214184046	0.03879201	1.223819971	0.029070109	1.393437028	0.01111761

Table 2B. Down regulated proteins identified in Volcano plots with fold change and p-values relative to ADSCs

Accession and gene name	Protein name	12 hr:ADSC fold change	12 hr:ADSC p-value	24 hr:ADSC fold change	24 hr:ADSC p-value	GBC:ADSC fold change	GBC:ADSC p-value
Proteins only in 12 hr differentiation							
sp|P04406|G3P_HUMAN	Glyceraldehyde-3-phosphate dehydrogenase	0.8479277	0.0043422	0.8963611	0.0539365	1.29605	0.0126654
sp|P06733|ENOA_HUMAN	Alpha-enolase	0.8004785	0.003791	0.8899997	0.0494512	0.8673062	0.0889979
sp|Q16658|FSCN1_HUMAN	Fascin	0.8632113	0.0081369	0.9985458	0.9725319	0.9803382	0.7522615
sp|P62258|1433E_HUMAN	14-3-3 protein epsilon	0.7345669	0.0014579	0.7889716	0.0540487	2.7000389	1.51E-08
sp|P63244|GBLP_HUMAN	Guanine nucleotide-binding protein subunit beta-2-like 1	0.7850113	0.0023291	1.026148	0.7182648	0.9216409	0.2950645
sp|P08238|HS90B_HUMAN	Heat shock protein HSP 90-beta	0.7536395	0.0140655	0.860231	0.1114735	0.9950555	0.9490238
sp|P62701|RS4X_HUMAN	40S ribosomal protein S4, X isoform	0.7593142	0.0005935	1.144268	0.2589218	1.1194659	0.2733781
sp|P09651|ROA1_HUMAN	Heterogeneous nuclear ribonucleoprotein A1	0.7305018	0.0051622	1.106936	0.3859383	2.0843611	0.0006238
sp|P61247|RS3A_HUMAN	40S ribosomal protein S3a	0.836074	0.049875	1.03742	0.4289024	1.320195	0.001181
sp|Q9Y617|SERC_HUMAN	Phosphoserine aminotransferase	0.7837498	0.0029119	0.8880233	0.135478	1.087113	0.2114475
sp|P30041|PRDX6_HUMAN	Peroxiredoxin-6	0.7284337	0.0064425	0.7679175	0.0504089	1.132565	0.0761582
sp|P63104|1433Z_HUMAN	14-3-3 protein zeta/delta	0.7794408	0.0424038	0.8261315	0.1741135	1.9782979	3.104E-05
sp|P08865|RSSA_HUMAN	40S ribosomal protein SA	0.7462529	0.0099222	1.036908	0.5412839	0.9988793	0.9859492
sp|P62937|PPIA_HUMAN	Peptidyl-prolyl cis-trans isomerase A	0.7663312	0.0020865	1.062439	0.3747487	2.0133979	0.0001145
sp|Q13347|EIF3I_HUMAN	Eukaryotic translation initiation factor 3 subunit I	0.8121918	0.0102658	0.9462903	0.3618241	1.018685	0.8342772
sp|O75534|CSDE1_HUMAN	Cold shock domain-containing protein E1	0.771526	0.0034917	0.9900259	0.8615462	0.9455857	0.6485646
sp|P30050|RL12_HUMAN	60S ribosomal protein L12	0.849311	0.0232884	1.0797631	0.2055826	0.8181012	0.0908025
sp|P55786|PSA_HUMAN	Puromycin-sensitive aminopeptidase	0.4095355	0.0208944	0.8498592	0.2518263	1.940941	0.0009965

Table 2B. Continued

Accession and Gene name	Protein Name	12 hr:ADSC fold change	12 hr:ADSC p-value	24 hr:ADSC fold change	24 hr:ADSC p-value	GBC:ADSC fold change	GBC:ADSC p-value
sp|P02511|CRYAB_HUMAN	Alpha-crystallin B chain	0.6343505	0.0032148	1.02856	0.685686	1.220765	0.0158245
sp|P30044|PRDX5_HUMAN	Peroxiredoxin-5, mitochondrial	0.7028021	0.0389368	0.8285266	0.1052497	0.8535319	0.1997427
sp|P62328|TYB4_HUMAN	Thymosin beta-4	0.4920007	0.0332198	0.8621768	0.2507035	1.239386	0.4872846
sp|P63220|RS21_HUMAN	40S ribosomal protein S21	0.7481042	0.0084351	1.052633	0.6723817	0.8575014	0.073444
sp|P18085|ARF4_HUMAN	ADP-ribosylation factor 4	0.6821533	0.0280265	0.9178579	0.79254	0.8463399	0.4097828
sp|P18621|RL17_HUMAN	60S ribosomal protein L17	0.6151012	0.0349046	1.057725	0.5479587	0.6039299	0.0704918
sp|P16949|STMN1_HUMAN	Stathmin	0.8414626	0.0448395	0.985819	0.8424742	2.1492679	1.178E-05
sp|Q9NR30|DDX21_HUMAN	Nucleolar RNA helicase 2	0.743278	0.0099099	0.9631584	0.8492183	0.5311144	0.0828007
sp|P49773|HINT1_HUMAN	Histidine triad nucleotide-binding protein 1	0.7960001	0.0157561	0.9326981	0.5084993	1.8662699	0.0207274
sp|Q96JY6|PDLI2_HUMAN	PDZ and LIM domain protein 2	0.7705169	0.0181184	0.8789578	0.3594843	0.5489806	0.0511937
sp|P09669|COX6C_HUMAN	Cytochrome c oxidase subunit 6C	0.6379359	0.013377	1.116226	0.2616933	0.9925451	0.9516448
sp|P30520|PURA2_HUMAN	Adenylosuccinate synthetase isozyme 2	0.7602439	0.0369208	0.9035071	0.2785547	0.8973022	0.4219353
sp|P06493|CDK1_HUMAN	Cyclin-dependent kinase 1	0.7085927	0.0163401	0.7424781	0.1200113	2.3315251	0.0133933
sp|P00403|COX2_HUMAN	Cytochrome c oxidase subunit 2	0.5474085	0.0229093	0.8213091	0.1686617	1.686554	0.0307677
sp|Q9H910|HN1L_HUMAN	Hematological and neurological expressed 1-like protein	0.7686939	0.0395484	0.9141212	0.2472908	1.1195869	0.4445185
sp|Q13308|PTK7_HUMAN	Inactive tyrosine-protein kinase 7	0.7176057	0.0155243	0.7806843	0.2195718	0.8202866	0.2265889
sp|Q8N3F8|MILK1_HUMAN	MICAL-like protein 1	0.6290908	0.0317877	0.9276105	0.4822235	1.50721	0.0750358
sp|Q96K17|BT3L4_HUMAN	Transcription factor BTF3 homolog 4	0.6892197	0.0486006	0.6607736	0.1085802	0.496424	0.112247
Common Proteins in 12 and 24 hr differentiation							
sp|P06744|G6PI_HUMAN	Glucose-6-phosphate isomerase	0.7193677	0.0006254	0.6672136	8.246E-05	2.2487891	1.036E-08
sp|Q9NZU5|LMCD1_HUMAN	LIM and cysteine-rich domains protein 1	0.7071645	0.0004705	0.6401113	4.341E-08	2.296283	2.267E-09
sp|P60174|TPIS_HUMAN	Triosephosphate isomerase	0.7501674	0.0113529	0.7045917	0.0004007	2.5271809	6.364E-08
sp|P49588|SYAC_HUMAN	Alanine–tRNA ligase, cytoplasmic	0.6795498	5.394E-05	0.5746737	3.913E-06	1.371278	4.908E-05
sp|P04792|HSPB1_HUMAN	Heat shock protein beta-1	0.5604951	0.0001762	0.7426677	0.0209271	1.541172	0.0089136
sp|P35222|CTNB1_HUMAN	Catenin beta-1	0.8595872	0.0128006	0.7611314	1.582E-05	0.8387557	0.1275463
sp|P36871|PGM1_HUMAN	Phosphoglucomutase-1	0.7463383	0.0001896	0.6675955	6.797E-05	0.9217962	0.1677606
sp|Q15417|CNN3_HUMAN	Calponin-3	0.5205765	0.0011651	0.5401105	0.0003287	3.3978031	1.723E-06
sp|P62979|RS27A_HUMAN	Ubiquitin-40S ribosomal protein S27a	0.5051308	0.0128211	0.6933423	0.0414675	1.412729	0.1300915
sp|P35613|BASI_HUMAN	Basigin	0.7667562	0.0006819	0.786752	0.0052719	1.478635	8.056E-05
sp|P00966|ASSY_HUMAN	Argininosuccinate synthase	0.6765513	0.0031044	0.6359119	0.0020193	2.331908	3.533E-06
sp|Q12841|FSTL1_HUMAN	Follistatin-related protein 1	0.7639553	0.0345735	0.5640365	0.0190533	1.070824	0.5687613
sp|P07437|TBB5_HUMAN	Tubulin beta chain	0.4618195	0.0499191	0.5135489	0.0062117	0.9821569	0.9072029
sp|P17936|IBP3_HUMAN	Insulin-like growth factor-binding protein 3	0.5418074	0.0067458	0.4080258	0.0063709	0.3198267	0.0523204
sp|P50579|AMPM2_HUMAN	Methionine aminopeptidase 2	0.7693873	0.0483193	0.6800565	0.0174458	0.938477	0.4942554
sp|O15427|MOT4_HUMAN	Monocarboxylate transporter 4	0.6468069	0.0497313	0.6395898	0.0477522	0.1273622	0.0785593
sp|Q9BV57|MTND_HUMAN	1,2-dihydroxy-3-keto-5-methylthiopentene dioxygenase	0.5140472	0.002501	0.4079044	0.004841	2.0234301	0.0111199
sp|Q92896|GSLG1_HUMAN	Golgi apparatus protein 1	0.6584018	0.0078619	0.5889162	0.0004774	0.8151252	0.1259657

Table 2B. Continued

Accession and Gene name	Protein Name	12 hr:ADSC fold change	12 hr:ADSC p-value	24 hr:ADSC fold change	24 hr:ADSC p-value	GBC:ADSC fold change	GBC:ADSC p-value
sp|P28300|LYOX_HUMAN	Protein-lysine 6-oxidase	0.6829536	0.0262415	0.3348025	0.0257906	0.3427074	0.226561
Proteins only in 24 hr differentiation							
sp|Q16881|TRXR1_HUMAN	Thioredoxin reductase 1, cytoplasmic	1.0364439	0.3616807	0.8219741	0.0005493	0.9360311	0.1332849
sp|P48735|IDHP_HUMAN	Isocitrate dehydrogenase (NADP), mitochondrial	1.187354	0.001626	0.760787	0.0022276	4.9582028	3.073E-11
sp|P17858|K6PL_HUMAN	6-phosphofructokinase, liver type	0.8796898	0.4738032	0.8036854	0.0026158	0.7909461	0.1816241
sp|P49411|EFTU_HUMAN	Elongation factor Tu, mitochondrial	1.136111	0.0326502	0.7871462	0.0011592	1.947157	6.357E-07
sp|P20810|ICAL_HUMAN	Calpastatin	0.8750533	0.1081493	0.7568965	0.0196435	0.7850653	0.1937321
sp|P30086|PEBP1_HUMAN	Phosphatidylethanolamine-binding protein 1	0.8731124	0.0211942	0.8283793	0.0038564	3.1945789	1.385E-07
sp|P35237|SPB6_HUMAN	Serpin B6	0.8802679	0.1745626	0.8257262	0.0086406	0.9815652	0.7505975
sp|P07339|CATD_HUMAN	Cathepsin D	1.051528	0.4394175	0.8192881	0.0117687	1.546684	0.0010593
sp|Q92900|RENT1_HUMAN	Regulator of nonsense transcripts 1	0.9178929	0.2185951	0.8558482	0.027399	0.8075969	0.0586372
sp|P09960|LKHA4_HUMAN	Leukotriene A-4 hydrolase	0.9437257	0.5129562	0.8397065	0.049417	1.160228	0.2741844
sp|Q16822|PCKGM_HUMAN	Phosphoenolpyruvate carboxykinase (GTP), mitochondrial	0.9528816	0.8248823	0.5842852	0.0001355	0.6504104	0.0637888
sp|Q8N8S7|ENAH_HUMAN	Protein enabled homolog	0.8274177	0.0571576	0.6830815	0.0069704	0.9318953	0.5751261
sp|P07203|GPX1_HUMAN	Glutathione peroxidase 1	0.8624336	0.2153537	0.7866376	0.0186332	2.587467	0.001527
sp|Q99961|SH3G1_HUMAN	Endophilin-A2	0.8050464	0.0544368	0.8494079	0.0429622	0.8313006	0.2537356
sp|P63092|GNAS2_HUMAN	Guanine nucleotide-binding protein G(s) subunit alpha isoforms short	0.8557481	0.1282786	0.8180471	0.0324584	1.7606061	0.0025444
sp|P68400|CSK21_HUMAN	Casein kinase II subunit alpha	0.9240049	0.2656185	0.8457134	0.0444661	1.105554	0.3466572
sp|Q9BRK5|CAB45_HUMAN	45 kDa calcium-binding protein	0.5650094	0.1218079	0.5348625	0.0083942	1.283482	0.052236
sp|P08648|ITA5_HUMAN	Integrin alpha-5	0.8827975	0.283567	0.8334129	0.0390296	0.2592828	0.1002662
sp|Q04760|LGUL_HUMAN	Lactoylglutathione lyase	0.8773558	0.1461125	0.767711	0.031137	2.81745	0.0119689
sp|P25325|THTM_HUMAN	3-mercaptopyruvate sulfurtransferase	0.9139439	0.4899827	0.6435751	0.0176827	1.033338	0.784981
sp|Q8IVL6|P3H3_HUMAN	Prolyl 3-hydroxylase 3	0.8073167	0.2868669	0.5731455	0.0264081	0.3668924	0.0672391
sp|Q9HB07|MYG1_HUMAN	UPF0160 protein MYG1, mitochondrial	0.8819175	0.6004307	0.622142	0.0089968	1.078177	0.7573638
sp|P10619|PPGB_HUMAN	Lysosomal protective protein	0.8569001	0.4883563	0.6964424	0.0469068	0.9313151	0.868605
sp|P52888|THOP1_HUMAN	Thimet oligopeptidase	0.9622395	0.7386975	0.837072	0.0478316	1.31484	0.3072187
sp|O96013|PAK4_HUMAN	Serine/threonine-protein kinase PAK 4	1.0217381	0.8920609	0.6765835	0.0410042	1.333773	0.5003013
sp|Q8ND76|CCNY_HUMAN	Cyclin-Y	0.8020011	0.216727	0.65859	0.0363463	0.8060961	0.4418439
Common Proteins in 24 hr differentiation and GBCs							
sp|P02751|FINC_HUMAN	Fibronectin	1.05277	0.1802123	0.4407711	5.836E-19	0.1742529	1.563E-18
sp|Q01995|TAGL_HUMAN	Transgelin	0.6692728	0.0876543	0.6856616	0.0109215	0.0669862	0.0001268
sp|O43795|MYO1B_HUMAN	Unconventional myosin-Ib	1.024282	0.5635512	0.8692154	0.0026827	0.3533631	3.264E-06
sp|Q9NZN4|EHD2_HUMAN	EH domain-containing protein 2	0.9012447	0.0739072	0.65933	0.0001831	0.2320304	5.896E-06
sp|Q07954|LRP1_HUMAN	Prolow-density lipoprotein receptor-related protein 1	0.8714587	0.0038484	0.6779363	5.012E-08	0.7306147	0.0002078
sp|Q9H4M9|EHD1_HUMAN	EH domain-containing protein 1	0.9417256	0.2532193	0.8380113	0.000365	0.5321978	5.697E-06

Table 2B. Continued

Accession and Gene name	Protein Name	12 hr:ADSC fold change	12 hr:ADSC p-value	24 hr:ADSC fold change	24 hr:ADSC p-value	GBC:ADSC fold change	GBC:ADSC p-value
sp|P80723|BASP1_HUMAN	Brain acid soluble protein 1	0.9116059	0.1819695	0.7202799	0.0410783	0.0676923	1.521E-07
sp|P04844|RPN2_HUMAN	Dolichyl-diphosphooligosaccharide–protein glycosyltransferase subunit 2	0.9017079	0.2878655	0.8192101	0.0399242	0.4075336	0.0022847
sp|P30837|AL1B1_HUMAN	Aldehyde dehydrogenase X, mitochondrial	0.9417027	0.3682509	0.670727	0.001719	0.3164505	0.0001068
sp|Q6WCQ1|MPRIP_HUMAN	Myosin phosphatase Rho-interacting protein	0.9359979	0.2837241	0.801344	0.0029636	0.5354406	0.0075895
sp|Q15063|POSTN_HUMAN	Periostin	1.500139	0.0001878	0.5885563	0.0010843	0.3422702	0.0043296
sp|P54727|RD23B_HUMAN	UV excision repair protein RAD23 homolog B	0.8896854	0.1443552	0.7950544	0.0151775	0.6107698	0.0002073
sp|P68032|ACTC_HUMAN	Actin, alpha cardiac muscle 1	0.5544822	0.1149586	0.5408995	0.0260236	0.3912214	0.0114004
sp|P98082|DAB2_HUMAN	Disabled homolog 2	0.9615206	0.6100879	0.7754198	0.0185135	0.3850327	0.0200069
sp|P12111|CO6A3_HUMAN	Collagen alpha-3 (VI) chain	1.334669	0.0003428	0.8098702	0.0016986	0.3830687	0.0017061
sp|Q969G5|PRDBP_HUMAN	Protein kinase C delta-binding protein	0.9411212	0.5362816	0.8662521	0.049586	0.2927489	6.347E-05
sp|P62070|RRAS2_HUMAN	Ras-related protein R-Ras2	0.8131321	0.1026654	0.7656406	0.04193	0.4747174	0.0066609
sp|Q96KP4|CNDP2_HUMAN	Cytosolic non-specific dipeptidase	0.9173274	0.410962	0.7831527	0.0147257	0.7192879	0.0329394
sp|Q15758|AAAT_HUMAN	Neutral amino acid transporter B(0)	1.041995	0.5513352	0.8404037	0.0433146	0.6372434	0.0378501
sp|Q15582|BGH3_HUMAN	Transforming growth factor-beta-induced protein ig-h3	0.9638007	0.7168077	0.4342145	0.0015891	0.193604	0.0083622
sp|Q9Y570|PPME1_HUMAN	Protein phosphatase methylesterase 1	0.8078368	0.0714756	0.7711414	0.0079941	0.6471239	0.0051838
sp|Q9NRV9|HEBP1_HUMAN	Heme-binding protein 1	0.7728173	0.053967	0.7515048	0.024625	0.2896793	0.0215531
sp|Q9UBG0|MRC2_HUMAN	C-type mannose receptor 2	0.7810244	0.1127253	0.6724297	0.0199727	0.3234429	0.01084
sp|O14495|LPP3_HUMAN	Lipid phosphate phosphohydrolase 3	0.7414259	0.1132276	0.711651	0.0106689	0.1977974	0.0078443
sp|P08473|NEP_HUMAN	Neprilysin	0.8780729	0.3033772	0.6565581	0.0029237	0.2834384	0.0031473
sp|O00461|GOLI4_HUMAN	Golgi integral membrane protein 4	0.9204073	0.406372	0.7727606	0.0378564	0.7051854	0.0251325
sp|Q16270|IBP7_HUMAN	Insulin-like growth factor-binding protein 7	0.340861	0.0689417	0.3130495	0.0357396	0.1773682	0.0483662
Common Proteins in 12 hr differentiation and GBCs							
sp|P35579|MYH9_HUMAN	Myosin-9	0.8423561	1.212E-07	0.9585411	0.204614	0.1792233	1.745E-39
sp|P14618|KPYM_HUMAN	Pyruvate kinase isozymes M1/M2	0.7591904	0.001561	0.9149806	0.1026978	0.6729065	5.251E-05
sp|P13639|EF2_HUMAN	Elongation factor 2	0.7993308	2.653E-05	0.9536575	0.2111206	0.6309205	9.996E-09
sp|P30101|PDIA3_HUMAN	Protein disulfide-isomerase A3	0.7731736	8.563E-05	1.065763	0.2355234	0.5595611	4.566E-10
sp|Q07065|CKAP4_HUMAN	Cytoskeleton-associated protein 4	0.8585722	0.0056568	1.09707	0.0344548	0.6766971	1.092E-06
sp|P09493|TPM1_HUMAN	Tropomyosin alpha-1 chain	0.3823238	0.0089529	0.7206582	0.1853321	0.1964161	0.0019547
sp|P36578|RL4_HUMAN	60S ribosomal protein L4	0.7818362	0.0121028	0.8841913	0.1588947	0.5938498	0.00011
sp|Q15084|PDIA6_HUMAN	Protein disulfide-isomerase A6	0.8253382	0.0353444	1.105119	0.1535215	0.5150038	0.000791
sp|P67936|TPM4_HUMAN	Tropomyosin alpha-4 chain	0.6354412	0.0050757	0.9631136	0.873189	0.4140534	0.0004444
sp|Q9NR12|PDLI7_HUMAN	PDZ and LIM domain protein 7	0.8502656	0.0033457	0.9716707	0.7257622	0.2132873	4.529E-06
sp|P62424|RL7A_HUMAN	60S ribosomal protein L7a	0.6631073	0.0090768	0.9861412	0.8999533	0.6202911	0.0028769
sp|Q9ULV4|COR1C_HUMAN	Coronin-1C	0.8000384	0.003047	0.8927166	0.0218495	0.2160703	2.519E-07
sp|P26641|EF1G_HUMAN	Elongation factor 1-gamma	0.7462852	0.0186326	1.047043	0.4670203	0.6336192	0.0009937
sp|P18124|RL7_HUMAN	60S ribosomal protein L7	0.7980775	0.0165588	1.04485	0.6165355	0.5023291	8.299E-05
sp|Q02878|RL6_HUMAN	60S ribosomal protein L6	0.7674008	0.0030989	0.8946929	0.0621624	0.5335739	3.795E-06

Table 2B. Continued

Accession and Gene name	Protein Name	12 hr:ADSC fold change	12 hr:ADSC p-value	24 hr:ADSC fold change	24 hr:ADSC p-value	GBC:ADSC fold change	GBC:ADSC p-value
sp|O15144|ARPC2_HUMAN	Actin-related protein 2/3 complex subunit 2	0.7838175	0.0044124	0.9419952	0.5304531	0.5372279	6.401E-05
sp|P60660|MYL6_HUMAN	Myosin light polypeptide 6	0.7616986	0.0495097	1.068398	0.2886685	0.5832632	0.0147406
sp|Q15293|RCN1_HUMAN	Reticulocalbin-1	0.6665307	0.0002087	0.8986852	0.0508759	0.1602958	4.174E-08
sp|Q96HC4|PDLI5_HUMAN	PDZ and LIM domain protein 5	0.5892135	0.0008179	0.8770573	0.5314806	0.2118111	5.798E-06
sp|P46781|RS9_HUMAN	40S ribosomal protein S9	0.7164086	0.0056955	1.013286	0.8541168	0.6084469	0.0008322
sp|P62241|RS8_HUMAN	40S ribosomal protein S8	0.723499	0.008818	1.1233	0.1691011	0.7230386	0.0046592
sp|Q8TDX7|NEK7_HUMAN	Serine/threonine-protein kinase Nek7	0.8028638	0.0005725	0.8820205	0.0219638	0.2457737	5.175E-07
sp|P63241|IF5A1_HUMAN	Eukaryotic translation initiation factor 5A-1	0.804385	0.0316132	1.133515	0.2812248	0.5861024	0.0029435
sp|P24844|MYL9_HUMAN	Myosin regulatory light polypeptide 9	0.771409	0.0317043	0.845117	0.0967934	0.2045051	0.0099072
sp|P39019|RS19_HUMAN	40S ribosomal protein S19	0.6352447	0.0016217	1.0988491	0.2598861	0.6985727	0.0125732
sp|P62249|RS16_HUMAN	40S ribosomal protein S16	0.858236	0.0042911	1.211066	0.0024016	0.7129009	1.012E-05
sp|P21291|CSRP1_HUMAN	Cysteine and glycine-rich protein 1	0.5783014	0.0076937	0.7048385	0.0751373	0.1401316	0.0004225
sp|P62750|RL23A_HUMAN	60S ribosomal protein L23a	0.6930985	0.0008642	1.189059	0.0170376	0.4874163	0.0005725
sp|P07737|PROF1_HUMAN	Profilin-1	0.735016	0.0374251	1.066458	0.2291982	0.3612709	0.0009833
sp|P27635|RL10_HUMAN	60S ribosomal protein L10	0.7687711	0.0078934	0.9977811	0.9774836	0.7807455	0.0424448
sp|P62244|RS15A_HUMAN	40S ribosomal protein S15a	0.6297469	0.0310408	1.2447751	0.2475055	0.3974015	0.006189
sp|P40261|NNMT_HUMAN	Nicotinamide N-methyltransferase	0.4948544	0.0145719	0.6104929	0.089145	0.4008726	0.0055721
sp|O75396|SC22B_HUMAN	Vesicle-trafficking protein SEC22b	0.8383446	0.0477434	0.9134793	0.2489925	0.6230699	0.0051087
sp|P63000|RAC1_HUMAN	Ras-related C3 botulinum toxin substrate 1	0.7182943	0.0425175	0.9622406	0.6886851	0.4670397	0.0072975
sp|P52565|GDIR1_HUMAN	Rho GDP-dissociation inhibitor 1	0.6346489	0.0200063	0.9114226	0.2442628	0.5560255	0.0041023
sp|Q02543|RL18A_HUMAN	60S ribosomal protein L18a	0.7989309	0.0054508	0.9987536	0.99314	0.5924663	0.001603
sp|P31949|S10AB_HUMAN	Protein S100-A11	0.7316054	0.0105927	0.9486079	0.454312	0.5093769	0.0051478
sp|Q9NUQ6|SPS2L_HUMAN	SPATS2-like protein	0.8603883	0.0377549	0.8679588	0.4357617	0.6844587	0.0203066
sp|Q9UBY9|HSPB7_HUMAN	Heat shock protein beta-7	0.5591881	0.0039141	0.8718413	0.1764828	0.1434866	0.0124455
sp|P62851|RS25_HUMAN	40S ribosomal protein S25	0.7520575	0.0210642	1.257262	0.0216226	0.640693	0.0285225
sp|P60866|RS20_HUMAN	40S ribosomal protein S20	0.5922481	0.0372282	1.135938	0.1952282	0.5971945	0.0331289
sp|Q15121|PEA15_HUMAN	Astrocytic phosphoprotein PEA-15	0.7424016	0.0342224	0.8453032	0.2365656	0.5568212	0.01295
sp|Q07020|RL18_HUMAN	60S ribosomal protein L18	0.7694229	0.0284774	0.9228408	0.3425165	0.3917271	0.0355194
sp|P10599|THIO_HUMAN	Thioredoxin	0.6320711	0.0364051	1.015246	0.849784	0.3958604	0.0290566
sp|P04080|CYTB_HUMAN	Cystatin-B	0.6261729	0.0164924	0.7203438	0.1116478	0.5600607	0.0261583
sp|Q99584|S10AD_HUMAN	Protein S100-A13	0.6776413	0.0141411	0.936109	0.683051	0.4091621	0.0109403
sp|Q96FQ6|S10AG_HUMAN	Protein S100-A16	0.7541828	0.0181902	0.7892096	0.1416664	0.4442775	0.0107498
sp|Q9UK76|HN1_HUMAN	Hematological and neurological expressed 1 protein	0.6930878	0.0069185	0.8315814	0.0583053	0.6368985	0.0217168
sp|Q9Y281|COF2_HUMAN	Cofilin-2	0.7557867	0.0425518	0.79008	0.2477008	0.411954	0.0016992
sp|P07951|TPM2_HUMAN	Tropomyosin beta chain	0.2181936	0.0301534	0.3476089	0.1504305	0.1699484	0.0294093
Common Proteins in 12, 24 and GBCs							
sp|P21333|FLNA_HUMAN	Filamin-A	0.6491441	1.197E-20	0.775251	3.467E-08	0.2333875	0
sp|Q14315|FLNC_HUMAN	Filamin-C	0.691992	1.206E-23	0.8109596	5.152E-08	0.1362745	9.121E-29

Table 2B. Continued

Accession and Gene name	Protein Name	12 hr:ADSC fold change	12 hr:ADSC p-value	24 hr:ADSC fold change	24 hr:ADSC p-value	GBC:ADSC fold change	GBC:ADSC p-value
sp|O75369|FLNB_HUMAN	Filamin-B	0.8066565	4.197E-13	0.8043511	4.036E-16	0.2220095	6.755E-27
sp|O43707|ACTN4_HUMAN	Alpha-actinin-4	0.7782484	5.953E-08	0.825819	6.121E-06	0.5644021	7.637E-12
sp|P02452|CO1A1_HUMAN	Collagen alpha-1(I) chain	0.1710951	9.168E-08	0.1382745	1.707E-13	0.0871599	1.366E-13
sp|P08133|ANXA6_HUMAN	Annexin A6	0.7843405	5.397E-05	0.8396946	8.225E-05	0.1753338	1.19E-12
sp|Q05682|CALD1_HUMAN	Caldesmon	0.6998289	1.765E-06	0.8143998	0.0014214	0.4336191	1.744E-09
sp|P07355|ANXA2_HUMAN	Annexin A2	0.7777895	0.0138044	0.8567227	0.0063894	0.6411493	9.041E-05
sp|P12814|ACTN1_HUMAN	Alpha-actinin-1	0.791617	0.0101087	0.7677427	0.0018612	0.1750646	2.284E-09
sp|P08123|CO1A2_HUMAN	Collagen alpha-2 (I) chain	0.2235407	4.04E-08	0.1855634	2.282E-12	0.1483753	3.537E-10
sp|P13797|PLST_HUMAN	Plastin-3	0.6665052	6.952E-07	0.68303	0.0014106	0.155993	1.821E-11
sp|P04075|ALDOA_HUMAN	Fructose-bisphosphate aldolase A	0.7604178	0.0073406	0.8671005	0.0114424	0.7167717	0.0005067
sp|P00558|PGK1_HUMAN	Phosphoglycerate kinase 1	0.5859095	0.0001153	0.6541614	8.688E-07	0.6226673	4.852E-07
sp|P08729|K2C7_HUMAN	Keratin, type II cytoskeletal 7	0.3680029	3.277E-09	0.5083517	3.862E-10	0.0634308	4.792E-08
sp|P04083|ANXA1_HUMAN	Annexin A1	0.7572839	0.0002047	0.8503217	0.0470738	0.550002	1.28E-07
sp|P07996|TSP1_HUMAN	Thrombospondin-1	0.7980919	0.000262	0.553084	7.377E-09	0.2897949	1.053E-07
sp|P05783|K1C18_HUMAN	Keratin, type I cytoskeletal 18	0.4164745	1.808E-06	0.4301328	6.1E-07	0.1056535	4.488E-08
sp|O75083|WDR1_HUMAN	WD repeat-containing protein 1	0.6917547	4.643E-06	0.7336982	0.0007094	0.3800338	1.092E-10
sp|Q99715|COCA1_HUMAN	Collagen alpha-1 (XII) chain	0.3545905	1.41E-13	0.2877428	4.501E-18	0.2026522	6.706E-15
sp|Q96AC1|FERM2_HUMAN	Fermitin family homolog 2	0.7950298	7.873E-06	0.8533728	0.0033112	0.2169133	1.367E-10
sp|Q15942|ZYX_HUMAN	Zyxin	0.7646767	0.001499	0.8185034	0.0001323	0.1502384	7.344E-10
sp|O43852|CALU_HUMAN	Calumenin	0.5774046	9.216E-06	0.8483972	0.0222098	0.4965094	0.0002066
sp|P13674|P4HA1_HUMAN	Prolyl 4-hydroxylase subunit alpha-1	0.6946718	2.918E-06	0.6132792	1.034E-05	0.2874632	5.012E-08
sp|O15460|P4HA2_HUMAN	Prolyl 4-hydroxylase subunit alpha-2	0.6696345	3.711E-07	0.5143549	9.348E-08	0.2669969	3.101E-10
sp|P42224|STAT1_HUMAN	Signal transducer and activator of transcription 1-alpha/beta	0.8499698	0.0053961	0.7854432	0.0005595	0.4379452	5.75E-10
sp|Q99536|VAT1_HUMAN	Synaptic vesicle membrane protein VAT-1 homolog	0.8316366	0.0180953	0.8146253	0.0168569	0.2068785	0.0002163
sp|Q9UHB6|LIMA1_HUMAN	LIM domain and actin-binding protein 1	0.7435201	2.34E-05	0.7350705	0.0005448	0.3019533	1.856E-08
sp|Q14847|LASP1_HUMAN	LIM and SH3 domain protein 1	0.6822608	0.0040097	0.8205906	0.0125213	0.3513746	1.928E-06
sp|Q9Y696|CLIC4_HUMAN	Chloride intracellular channel protein 4	0.6635472	0.0298623	0.6565596	0.0294536	0.259223	2.416E-06
sp|P18669|PGAM1_HUMAN	Phosphoglycerate mutase 1	0.6600341	0.0005784	0.7290849	0.000285	0.5737495	0.0001545
sp|Q16643|DREB_HUMAN	Drebrin	0.7486963	0.0013527	0.8171875	0.0228791	0.3356167	1.741E-07
sp|Q16222|UAP1_HUMAN	UDP-N-acetylhexosamine pyrophosphorylase	0.6732854	0.0001079	0.7852986	0.0005487	0.3712067	5.819E-07
sp|P02461|CO3A1_HUMAN	Collagen alpha-1 (III) chain	0.2201081	0.0004393	0.1852412	0.0001674	0.1235914	0.0007796
sp|O00469|PLOD2_HUMAN	Procollagen-lysine,2-oxoglutarate 5-dioxygenase 2	0.3010921	1.377E-05	0.3480398	1.46E-07	0.1949575	4.065E-06
sp|P12109|CO6A1_HUMAN	Collagen alpha-1 (VI) chain	0.4696823	8.107E-05	0.4169624	1.04E-06	0.7281033	0.001178
sp|O00151|PDLI1_HUMAN	PDZ and LIM domain protein 1	0.8575081	0.0064386	0.808583	0.0013904	0.7191794	0.0001499
sp|Q9BUF5|TBB6_HUMAN	Tubulin beta-6 chain	0.5307726	0.0061257	0.6090587	0.0079562	0.277919	0.0004736
sp|Q02818|NUCB1_HUMAN	Nucleobindin-1	0.8226624	0.0371084	0.663159	1.352E-05	0.6716899	0.0183368

Table 2B. Continued

Accession and Gene name	Protein Name	12 hr:ADSC fold change	12 hr:ADSC p-value	24 hr:ADSC fold change	24 hr:ADSC p-value	GBC:ADSC fold change	GBC:ADSC p-value
sp|O43399|TPD54_HUMAN	Tumor protein D54	0.6686246	0.005498	0.7417749	0.011344	0.4392767	1.561E-05
sp|P07858|CATB_HUMAN	Cathepsin B	0.7033579	0.014844	0.6877466	0.0012351	0.2995372	0.0003164
sp|Q99439|CNN2_HUMAN	Calponin-2	0.7122491	0.0170487	0.6706736	0.0230627	0.5064756	0.0001678
sp|Q02809|PLOD1_HUMAN	Procollagen-lysine,2-oxoglutarate 5-dioxygenase 1	0.8466675	0.0085338	0.8482934	0.002677	0.3619584	4.314E-05
sp|P17813|EGLN_HUMAN	Endoglin	0.5273556	0.004124	0.6475987	0.0055206	0.147541	0.0005594
sp|O15143|ARC1B_HUMAN	Actin-related protein 2/3 complex subunit 1B	0.697738	0.0270338	0.84576	0.0351022	0.2651682	0.0004373
sp|P12110|CO6A2_HUMAN	Collagen alpha-2 (VI) chain	0.6012068	0.0088132	0.3789701	0.0007036	0.3206771	0.0017214
sp|P21980|TGM2_HUMAN	Protein-glutamine gamma-glutamyltransferase 2	0.5693054	4.331E-05	0.627192	0.0004874	0.1962446	0.0002049
sp|P26373|RL13_HUMAN	60S ribosomal protein L13	0.6572507	0.0010244	0.7834665	0.0095265	0.6630557	0.0040335
sp|Q14192|FHL2_HUMAN	Four and a half LIM domains protein 2	0.7846096	0.0029767	0.8173597	0.0012308	0.2725918	0.0390995
sp|Q93052|LPP_HUMAN	Lipoma-preferred partner	0.7990149	0.0225724	0.8337976	0.0406539	0.292731	0.0001339
sp|Q16647|PTGIS_HUMAN	Prostacyclin synthase	0.8080279	0.0319709	0.7324285	0.0019337	0.263861	0.0002228
sp|O15371|EIF3D_HUMAN	Eukaryotic translation initiation factor 3 subunit D	0.864748	0.0383892	0.8346376	0.0167422	0.6714211	0.003605
sp|P51911|CNN1_HUMAN	Calponin-1	0.4608479	0.0003309	0.4437445	0.0019445	0.2158564	0.007823
sp|Q13642|FHL1_HUMAN	Four and a half LIM domains protein 1	0.4609712	0.0001142	0.5427488	0.0001992	0.2829264	1.591E-06
sp|P20908|CO5A1_HUMAN	Collagen alpha-1 (V) chain	0.379388	0.0068348	0.3544788	0.0003237	0.2353524	0.0026677
sp|O60568|PLOD3_HUMAN	Procollagen-lysine,2-oxoglutarate 5-dioxygenase 3	0.7638809	0.0008531	0.8055949	0.0047301	0.556466	0.0003241
sp|P26022|PTX3_HUMAN	Pentraxin-related protein PTX3	0.416522	0.0040385	0.2322244	0.000583	0.186485	0.0139001
sp|Q9H425|CA198_HUMAN	Uncharacterized protein C1orf198	0.631039	0.0133804	0.6294332	0.0089014	0.264752	0.0014479
sp|P09486|SPRC_HUMAN	SPARC	0.4096919	0.0060709	0.1639415	0.0023144	0.2305094	0.0028895
sp|P06756|ITAV_HUMAN	Integrin alpha-V	0.5613986	0.018194	0.6385075	0.0016505	0.482797	0.0014006
sp|O15173|PGRC2_HUMAN	Membrane-associated progesterone receptor component 2	0.8195758	0.0447193	0.8143579	0.041582	0.3442066	0.0120293
sp|P05121|PAI1_HUMAN	Plasminogen activator inhibitor 1	0.3748078	0.002411	0.2813975	0.0062054	0.1704524	0.0032371
sp|P11047|LAMC1_HUMAN	Laminin subunit gamma-1	0.7204638	0.0263982	0.8115935	0.047751	0.5165971	0.0042495
sp|P41567|EIF1_HUMAN	Eukaryotic translation initiation factor 1	0.5903546	0.0021622	0.5996968	0.0012622	0.8147202	0.0319759
sp|P05787|K2C8_HUMAN	Keratin, type II cytoskeletal 8	0.7084652	0.0319926	0.6759541	0.0142614	0.3713869	0.0315686
sp|P08729|K2C7_HUMAN	Keratin, type II cytoskeletal 7	0.3680029	3.277E-09	0.5083517	3.862E-10	0.0634308	4.792E-08
sp|P05787|K2C8_HUMAN	Keratin, type II cytoskeletal 8	0.7084652	0.0319926	0.6759541	0.0142614	0.3713869	0.0315686

Table 2C. Statistically significant neuronal and stress proteins expressed by induced stem cells at 12 and 24 hrs

	Accession number	Name	Accession number	Name
	Neurogenic related proteins		Stress and shock related proteins	
12 hour unique proteins	Q09666	Neuroblast differentiation-associated protein	P09601	Heme oxygenase
	O94925	Glutaminase	P48507	Glutamate–cysteine ligase regulatory subunit
	P12111	Collagen alpha-3 (VI) chain	P11413	Glucose-6-phosphate 1-dehydrogenase
	A1X283	SH3 and PX domain-containing protein 2B		
24 hour unique proteins	P23219	Prostaglandin G/H synthase 1	P23219	Prostaglandin G/H synthase 1
	P50402	Emerin (wnt pathway)	Q9Y547	Heat shock protein beta-11
12 and 24 hour common proteins			GRP75	Stress-70 protein
12 hours and GBC common proteins	P14136	Glial fibrillary acidic protein		
	P15559	NAD(P)H dehydrogenase (quinone) 1		
	Q2M2I8	AP2-associated protein kinase 1		
24 hours and GBC common proteins	Q06830	Peroxiredoxin-1	P04264	Keratin, type II cytoskeletal 1
	P09429	High mobility group protein B1	P04792	Heat shock protein beta-1
	P30048	Thioredoxin-dependent peroxide reductase	P61604	10 kDa heat shock protein, mitochondrial
	P15121	Aldose reductase		

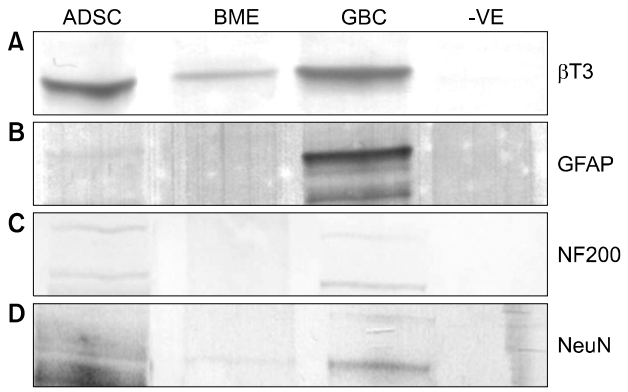

Fig. 4. (A) Western blot of BT3 positive in ADSCs, BME differentiated and GBCs seen at 55 kDa. (B) GFAP positively detected in GBCs at 48 kDa. (C) NF200 positively identified at 200 kDa in GBCs and very weakly in ADSC. (D) NeuN a very low positive in BME differentiated and GBCs. −VE is a negative control of a whole cell lysate of an unrelated cell line.

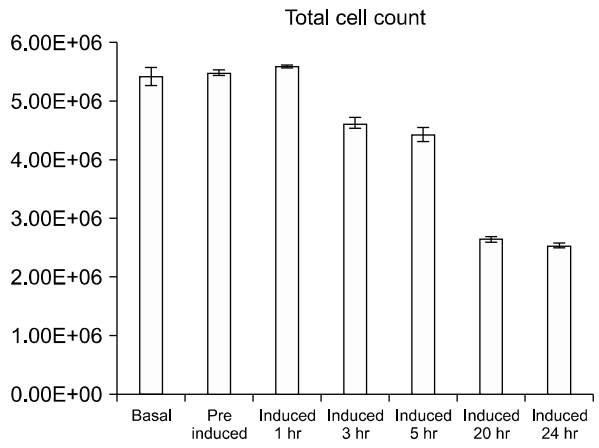

Fig. 5. Average total cell count at each time point over the BME treatment of ADSCs with mean error bars. Average cell count shows the total number of cells at each time point with drastic decreases in the final two points.

cfu/mm^2 or total population of 5.42E+06 cells. Subsequent to the BME treatment the population decreases by approximately 18% to 63 cfu/mm^2 by the 5 hour time point. After 20 hours the cell population decreases by 46%, to 35 cfu/mm^2, relative to the basal cells (Fig. 5). Upon harvest of the final time point the total dead/live ratio was 1:9 i.e. an average of 10% of cells were stained blue with trypan.

Bioplex

The Bioplex assay is an efficient system for examining up to 27 cytokines across multiple sample types simulta-

neously, revealing quantitative changes and relative concentrations of these secreted molecules. Media that the cells were growing in were collected and analysed from the differentiation time points 0, 1, 3, 5, 20 and 24 hours. A hierarchical clustering and Euclidean test in the DanteR software were used to cluster the multiple data points in a heat map configuration where red represents expression above median; green: expression below the median and Black: median expression across all samples (Fig. 6). The hierarchical clustering (Fig. 6) presents the cytokines with similar concentration trends over the differentiation time points.

Cytokines, while having their unique roles in metabolic and cellular processes, can often be regulated in synchrony or regulate the expression of other cytokines in MSCs (18). Individually and collectively their relative concentrations can be related to particular cellular events. As such a number of trends occur within the Bioplex temporal differentiation data set. The molecules IL-1ra, Eotaxin, IL-2 and Rantes share a uniform trend in this dataset with similar concentration fluctuations between IL-1ra and Eotaxin which are comparable to IL-2 and Rantes. The trend reveals the highest concentration of the respective molecules is present at the 0hr time point, with a uniform decrease to the lowest concentrations at the 1 hr time point. This is followed by a slight recovery at the 3rd through the 5th hr. The concentration decreases fractionally again at the 20th hr for IL-1ra and Eotaxin then stabilises at the final time point The next group of trend related cytokines were composed of IL-4, IL5, IL-9, MIP-1a and MIP-1b which followed a fairly simple and distinct trend. The highest concentration occurs at time point 0hrs which then decreases by approximately 75% for all five cytokines thereafter and remains comparatively at the similar concentrations for all time points, with a minor recovery at 3 hrs post induction (Supplementary Table 2). The group consisting of IL-7, IL-13, PDGF-bb, TNF-a, MCP, IFN-g have a somewhat similar trend to the previous group, in that the highest concentrations occur at time point 0hrs, the major defining trend for this series is the significant decrease in concentration to less than 10% in the next time point which is maintained over the course of the differentiation time showing a marginal increase at the 24 hour mark (Supplementary Table 2). The following group: IL-8, IL-10, IL-12, G-CSF and VEG-F also share some common features with the previous two groups in that the highest concentration is observable at time point 0 hrs. The difference is the substantial decrease to near non-detectable concentrations for the entirety of the differentiation (Supplementary Table 2). Conversely the two remaining cytokines IL-6 and FGF were grouped together due to their unique trends that appear to be somewhat related. The main difference between these trends in these two cytokines is that IL-6 appears to have a concentration below the detectable level at time point 0 hrs whereas FGF has approximately 42 pg/ml at the same time point. The trends display a somewhat similar trait after 1 hour with increasing concentrations in both cytokines with the highest levels at the final two time points (Supplementary Table 2).

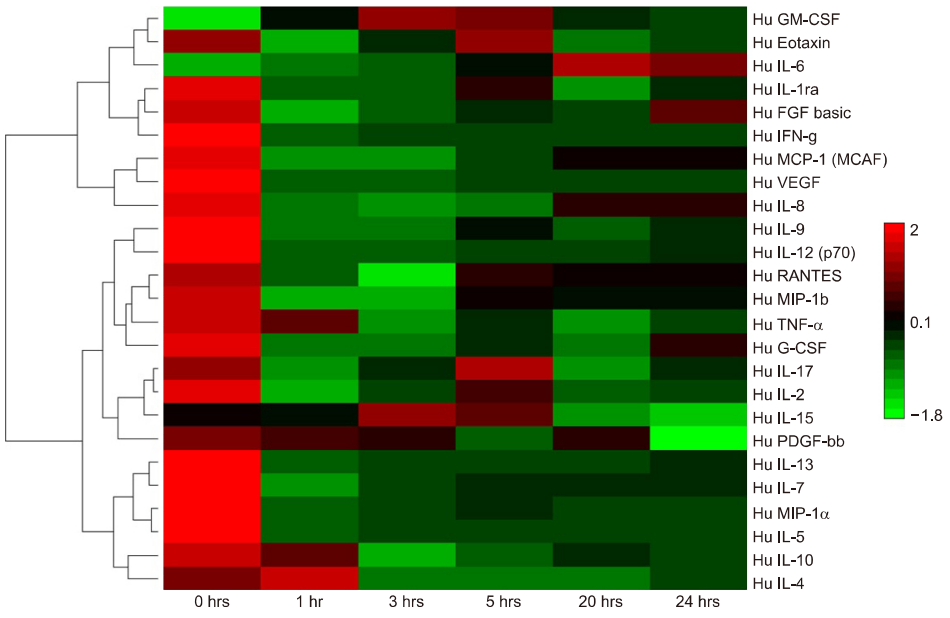

Fig. 6. Bioplex 27-plex cytokine array of ADSCs treated with BME over time. Bioplex comparisons of interleukins and cytokine secretions from basal ADSCs and temporal differentiation with BME neuronal differentiation media. Hierarchical clustering software and Euclidean test Red: expression above median; Green: expression below the median; Black: median expression across sample.

Discussion

In this study, we investigated hADSCs ability to transdifferentiate toward a neuronal-like lineage within 12 and 24 hours, as well as the changes in the proteome occurring during the differentiation process. It was found that the cells responded to BME differentiation media with similar morphological and marker profiles as previously reported (4, 5, 19) and several groups of proteins involved in neural growth and protection were identified by MS/MS analysis. We also found the acquired soluble proteome of hADSCs differentiated for 12 hours and 24 hours to be noticeably different from basal ADSCs and GBCs, presenting a number of fold changes in proteins related to neuronal differentiation, cytoskeletal remodeling as well as an array of stress response proteins. Furthermore Bioplex cytokine profiles present evidence of a large cellular remodeling shift and stress response activity during the induced differentiation process which is reflected in the proteomic data sets. This study reveals that the BME treatment of ADSCs toward a neurogenic lineage presents a wide array of neuronally related proteins and morphology however the extended exposure of BME to the cells induces a significant stress response.

As demonstrated in this work, the secreted material can be analysed via iTRAQ proteomics or Bioplex cytokine analysis for definitive profiling. Several stress and shock related proteins were identified (Table 2). The proteins Heme oxygenase, Glutamate--cysteine ligase regulatory subunit (GCLM), Glucose-6-phosphate 1-dehydrogenase (G6PD), Prostaglandin G/H synthase 1 (PTGS1), Heat shock protein beta-11 (HSPB11), Stress-70 protein (HSP-70), Keratin, type II cytoskeletal 1, Heat shock protein beta-1 (HSPB1) and 10 kDa heat shock protein (HSPE1), mitochondrial were all investigated to ascertain their role during induction as they were statistically significantly up regulated stress related proteins at the various time points.

The expression of Heme oxygenase (HO) in neurogenic induced ADSCs is an interesting finding since its primary function is the degradation of heme producing biliverdin, iron and carbon monoxide (20). The expression of HO has been found in lung epithelial and liver cell types experiencing oxidative stress (21, 22). Furthermore HO has annotated roles in the response to the action of the oxidative stress linked proinflammitory cytokines IL-1B and TNF-α in astroglial cells (23). It has also been found that HO and the proinflammatory cytokines play a protective role in neuronal cells experiencing oxidative stress as neurons over expressing HO are resistant to oxidative stress mediated cell death (24). The Bioplex results exhibited the expression of IL-1B and TNF-α was far too low for a discernible concentration to be calculated for the former and very low concentrations for the latter to elicit a proinflammatory affect (25). The expression of HO in neurogenic induced ADSCs is undoubtedly due to oxidative stress however the prevention of cell death was not apparent (Fig. 1). Its use as a potential marker indicating cellular distress and protection against oxidative induced death is useful in future studies to indicate stress in chemical inductions (24).

The expression of GCLM has also been linked to a response to oxidative stress; however it has also been detected in high concentrations in muscle cells and lung epithelium undergoing hypoxic or oxidative stress (26). Some studies have linked GCLM to improving the antioxidative defense in astroglial cells by enhancing hydrogen peroxide scavenging ability however this was also in the presence of a thyroid hormone (27), and modulation of the survival of astrocytes and neurons in the presence of reducing agents (28).

Similarly, the high expression of G6PD, like many of the other proteins in this cohort, has been linked to the oxidative stress response by maintaining a redox imbalance-induced apoptosis in a number of cell types (29). Studies in Parkinson's disease relating oxidative damage to neuronal cells in transgenic mice have shown a moderate increase in G6PD activity and an over expression and neuroprotective activity in aged animals (30).

Equally PTGS1 has been annotated by gene ontology to promote neuronal development and be induced due to oxidative stress. The mechanisms of which PTGS1 is expressed as a neuronal support protein or stress related protein are in response to different signals. The link PTGS1 has to neuronal development is directly associated with the moderate expression of the proinflammatory cytokines IL-1B and TNF-α (31), which in this study has been previously mentioned to have near undetectable concentrations. Studies into their expression during oxidative stress has shown a high expression of PTGS1 from various cell types in the presence of DMSO (32) which incidentally has also been used as an analogous neurogenic induction chemical (3, 4, 7).

Chemically induced oxidative stress to cells has been linked to inhibiting the COX-1 and COX-2 gene which directly affects the proliferation of cells and the high expression of PTGS1 (33). Our findings and the supportive literature indicates that the ADSCs treated with BME neurogenic induction media are responding in a similar manner to other cells types experiencing an overexposure to chemicals which cause an imbalance to the redox state

in cells.

Further, to the detected oxidative stress proteins, a variety of additional stress and shock related proteins were noteworthy to this study. HSPB11, which has been linked to an inflammatory response in certain diseases (34), was found to be uniquely and highly expressed in the 24 hour induced ADSCs with none of its ten annotated interacting partners detected in our datasets. Minimal literature is available on the investigation of HSPB11's role in the stress response. Its presence in the induced ASDCs cannot be accounted for except in response to inflammatory cytokines or due to the oxidative stress experienced by the cells.

HSP-70 is a widely studied heat shock protein and has been found to be ubiquitously expressed in all organisms, linked to the control of cellular proliferation and maintenance during aging (35). One study into homologous stress related proteins in *Mytilus edulis* have shown a differential in temperature determines the level and sites of expression of stress-70-like proteins in tissue (36). The over expression of HSP-70 has also been linked to the cell's response to toxic chemicals and the development of cancerous growth (37). The purpose of HSP-70 is postulated to be involved in the protection of cells under thermal or oxidative stress by inhibiting the aggregation of damaged and unfolded proteins (38).

Similarly, HSPB1 and HSPE1 expression is increased when cells are in distress which includes thermal, physical and chemical stressors (Table 2) (39). They are functionally similar to the HSP-70, also annotated in the inhibition of aggregating, damaged or stressed proteins (40). Thus the high expression of heat shock proteins reveals that the ADSCs are being exposed to a prolonged period in traumatic, stress inducing conditions.

Numerous of the above stress related proteins have been linked to the maintenance or protection of neuronal cells experiencing oxidative stress, the remaining shock induced proteins are not related to neuronal cells and are dually expressed due to the extensive stress. While these proteins functions are to preserve the cells in this environment, the loss of approximately 50% of the cell population is alarming and indicates that the surviving cells expressing the detected proteins may in fact be damaged by the induction process.

A shorter treatment may initiate the induction toward a neurogenic differentiation, as an exposure of more than 12 hours to the BME containing media is a stress inducing environment. Our findings essentially indicate that the produced cells may have had the potential for neurogenic differentiation due to the wide variety of neuronal related proteins expressed and detected. However the high abundance of up regulated stress related proteins and high cell death indicates the cells are being damaged. This suggests the culture conditions for inducing ADSCs toward a neurogenic linage with BME is not conducive to producing complete neuronal cells. Nonetheless, the process and mechanisms which drives the cells to differentiate is the most important result acquired as this could be mimicked with much milder and non-toxic chemical cocktails.

Conclusion

The use of chemical inducers to initiate neurogenesis has become well accepted because of its simplicity and due to its relatively rapid outcome of producing morphologically neuronal-like differentiated cells compared to the alternative growth factor induction methods. It is important that the choice of chemical inducer is not toxic to the cells to the extent that major cell death is apparent. While the use of BME produces interesting results in the induction of neurogenesis in ADSCs, it is quite toxic to cells and therefore would not be useful in a clinical setting. This is reflected in decrease in total cell population within the 24 hours of induction. The high death rate in the BME neurogenic induction would not be permissive for *in vivo* treatments, especially since the extent of damage or stress to the surviving cells has not been well characterised. A catalogue of stress proteins and potential markers can be useful in identifying the biological processes initiated during induced neurogenesis when utilising alternative chemicals to BME.

Acknowledgments

We would like to thank the Australian Proteome Analysis facility (APAF), Macquarie University, Thiri Zaw and Cameron Hill for technical support.

Potential conflict of Interest

The authors have no conflicting financial interest.

Supplementary Materials

Supplementary data including two tables can be found with this article online at http://pdf.medrang.co.kr/paper/pdf/IJSC/IJSC-10-s17036.pdf.

References

1. Arvidson K, Abdallah BM, Applegate LA, Baldini N, Cenni E, Gomez-Barrena E, Granchi D, Kassem M, Konttinen

YT, Mustafa K, Pioletti DP, Sillat T, Finne-Wistrand A. Bone regeneration and stem cells. J Cell Mol Med 2011; 15:718-746
2. Moraleda JM, Blanquer M, Bleda P, Iniesta P, Ruiz F, Bonilla S, Cabanes C, Tabares L, Martinez S. Adult stem cell therapy: dream or reality? Transpl Immunol 2006;17: 74-77
3. Lu P, Blesch A, Tuszynski MH. Induction of bone marrow stromal cells to neurons: differentiation, transdifferentiation, or artifact? J Neurosci Res 2004;77:174-191
4. Woodbury D, Schwarz EJ, Prockop DJ, Black IB. Adult rat and human bone marrow stromal cells differentiate into neurons. J Neurosci Res 2000;61:364-370
5. Zuk PA, Zhu M, Ashjian P, De Ugarte DA, Huang JI, Mizuno H, Alfonso ZC, Fraser JK, Benhaim P, Hedrick MH. Human adipose tissue is a source of multipotent stem cells. Mol Biol Cell 2002;13:4279-4295
6. Franco Lambert AP, Fraga Zandonai A, Bonatto D, Cantarelli Machado D, Pêgas Henriques JA. Differentiation of human adipose-derived adult stem cells into neuronal tissue: does it work? Differentiation 2009;77:221-228
7. Barnabé GF, Schwindt TT, Calcagnotto ME, Motta FL, Martinez G Jr, de Oliveira AC, Keim LM, D'Almeida V, Mendez-Otero R, Mello LE. Chemically-induced RAT mesenchymal stem cells adopt molecular properties of neuronal-like cells but do not have basic neuronal functional properties. PLoS One 2009;4:e5222
8. Unwin RD, Smith DL, Blinco D, Wilson CL, Miller CJ, Evans CA, Jaworska E, Baldwin SA, Barnes K, Pierce A, Spooncer E, Whetton AD. Quantitative proteomics reveals posttranslational control as a regulatory factor in primary hematopoietic stem cells. Blood 2006;107:4687-4694
9. Takahashi J, Palmer TD, Gage FH. Retinoic acid and neurotrophins collaborate to regulate neurogenesis in adult-derived neural stem cell cultures. J Neurobiol 1999;38:65-81
10. White K, Bruckner JV, Guess WL. Toxicological studies of 2-mercaptoethanol. J Pharm Sci 1973;62:237-241
11. Bunnell BA, Flaat M, Gagliardi C, Patel B, Ripoll C. Adipose-derived stem cells: isolation, expansion and differentiation. Methods 2008;45:115-120
12. Jobbins SE, Hill CJ, D'Souza-Basseal JM, Padula MP, Herbert BR, Krockenberger MB. Immunoproteomic approach to elucidating the pathogenesis of cryptococcosis caused by Cryptococcus gattii. J Proteome Res 2010;9: 3832-3841
13. Taverner T, Karpievitch YV, Polpitiya AD, Brown JN, Dabney AR, Anderson GA, Smith RD. DanteR: an extensible R-based tool for quantitative analysis of -omics data. Bioinformatics 2012;28:2404-2406
14. Quesnel C, Nardelli L, Piednoir P, Leçon V, Marchal-Somme J, Lasocki S, Bouadma L, Philip I, Soler P, Crestani B, Dehoux M. Alveolar fibroblasts in acute lung injury: biological behaviour and clinical relevance. Eur Respir J 2010;35:1312-1321
15. Yamauchi H, Miyamura K, Abo M. Proteomic assessment of important proteins for motor recovery in a rat model of photochemically-induced thrombosis. Journal of Applied Research 2009;9:139-147
16. Marangos PJ, Schmechel DE. Neuron specific enolase, a clinically useful marker for neurons and neuroendocrine cells. Annu Rev Neurosci 1987;10:269-295
17. Katsetos CD, Legido A, Perentes E, Mörk SJ. Class III beta-tubulin isotype: a key cytoskeletal protein at the crossroads of developmental neurobiology and tumor neuropathology. J Child Neurol 2003;18:851-866
18. Kilroy GE, Foster SJ, Wu X, Ruiz J, Sherwood S, Heifetz A, Ludlow JW, Stricker DM, Potiny S, Green P, Halvorsen YD, Cheatham B, Storms RW, Gimble JM. Cytokine profile of human adipose-derived stem cells: expression of angiogenic, hematopoietic, and pro-inflammatory factors. J Cell Physiol 2007;212:702-709
19. Safford KM, Hicok KC, Safford SD, Halvorsen YD, Wilkison WO, Gimble JM, Rice HE. Neurogenic differentiation of murine and human adipose-derived stromal cells. Biochem Biophys Res Commun 2002;294:371-379
20. Kikuchi G, Yoshida T, Noguchi M. Heme oxygenase and heme degradation. Biochem Biophys Res Commun 2005; 338:558-567
21. Vile GF, Basu-Modak S, Waltner C, Tyrrell RM. Heme oxygenase 1 mediates an adaptive response to oxidative stress in human skin fibroblasts. Proc Natl Acad Sci U S A 1994;91:2607-2610
22. Motterlini R, Foresti R, Bassi R, Green CJ. Curcumin, an antioxidant and anti-inflammatory agent, induces heme oxygenase-1 and protects endothelial cells against oxidative stress. Free Radic Biol Med 2000;28:1303-1312
23. Mehindate K, Sahlas DJ, Frankel D, Mawal Y, Liberman A, Corcos J, Dion S, Schipper HM. Proinflammatory cytokines promote glial heme oxygenase-1 expression and mitochondrial iron deposition: implications for multiple sclerosis. J Neurochem 2001;77:1386-1395
24. Chen K, Gunter K, Maines MD. Neurons overexpressing heme oxygenase-1 resist oxidative stress-mediated cell death. J Neurochem 2000;75:304-313
25. Radtke S, Wüller S, Yang XP, Lippok BE, Mütze B, Mais C, de Leur HS, Bode JG, Gaestel M, Heinrich PC, Behrmann I, Schaper F, Hermanns HM. Cross-regulation of cytokine signalling: pro-inflammatory cytokines restrict IL-6 signalling through receptor internalisation and degradation. J Cell Sci 2010;123:947-959
26. Krzywanski DM, Dickinson DA, Iles KE, Wigley AF, Franklin CC, Liu RM, Kavanagh TJ, Forman HJ. Variable regulation of glutamate cysteine ligase subunit proteins affects glutathione biosynthesis in response to oxidative stress. Arch Biochem Biophys 2004;423:116-125
27. Dasgupta A, Das S, Sarkar PK. Thyroid hormone promotes glutathione synthesis in astrocytes by up regulation of glutamate cysteine ligase through differential stimulation of its catalytic and modulator subunit mRNAs. Free Radic Biol Med 2007;42:617-626
28. Lavoie S, Chen Y, Dalton TP, Gysin R, Cuénod M, Steullet P, Do KQ. Curcumin, quercetin, and tBHQ modulate glu-

tathione levels in astrocytes and neurons: importance of the glutamate cysteine ligase modifier subunit. J Neurochem 2009;108:1410-1422
29. Efferth T, Schwarzl SM, Smith J, Osieka R. Role of glucose-6-phosphate dehydrogenase for oxidative stress and apoptosis. Cell Death Differ 2006;13:527-528; author reply 529-530
30. Mejías R, Villadiego J, Pintado CO, Vime PJ, Gao L, Toledo-Aral JJ, Echevarría M, López-Barneo J. Neuroprotection by transgenic expression of glucose-6-phosphate dehydrogenase in dopaminergic nigrostriatal neurons of mice. J Neurosci 2006;26:4500-4508
31. O'Banion MK, Miller JC, Chang JW, Kaplan MD, Coleman PD. Interleukin-1 beta induces prostaglandin G/H synthase-2 (cyclooxygenase-2) in primary murine astrocyte cultures. J Neurochem 1996;66:2532-2540
32. Hollebeeck S, Raas T, Piront N, Schneider YJ, Toussaint O, Larondelle Y, During A. Dimethyl sulfoxide (DMSO) attenuates the inflammatory response in the in vitro intestinal Caco-2 cell model. Toxicol Lett 2011;206:268-275
33. Asmis L, Tanner FC, Sudano I, Lüscher TF, Camici GG. DMSO inhibits human platelet activation through cyclooxygenase-1 inhibition. A novel agent for drug eluting stents? Biochem Biophys Res Commun 2010;391:1629-1633
34. Benagiano M, D'Elios MM, Amedei A, Azzurri A, van der Zee R, Ciervo A, Rombolà G, Romagnani S, Cassone A, Del Prete G. Human 60-kDa heat shock protein is a target autoantigen of T cells derived from atherosclerotic plaques. J Immunol 2005;174:6509-6517
35. Morano KA. New tricks for an old dog: the evolving world of Hsp70. Ann N Y Acad Sci 2007;1113:1-14
36. Paul Chapple J, Smerdon GR, Hawkins AJS. Stress-70 protein induction in Mytilus edulis: Tissue-specific responses to elevated temperature reflect relative vulnerability and physiological function. Journal of Experimental Marine Biology and Ecology 1997;217:225-235
37. Ricaniadis N, Kataki A, Agnantis N, Androulakis G, Karakousis CP. Long-term prognostic significance of HSP-70, c-myc and HLA-DR expression in patients with malignant melanoma. Eur J Surg Oncol 2001;27:88-93
38. Lüders J, Demand J, Höhfeld J. The ubiquitin-related BAG-1 provides a link between the molecular chaperones Hsc70/Hsp70 and the proteasome. J Biol Chem 2000;275:4613-4617
39. Jakob U, Gaestel M, Engel K, Buchner J. Small heat shock proteins are molecular chaperones. J Biol Chem 1993;268:1517-1520
40. Kiang JG, Tsokos GC. Heat shock protein 70 kDa: molecular biology, biochemistry, and physiology. Pharmacol Ther 1998;80:183-201